Biochimica et Biophysica Acta 1837 (2014) 14–32

Contents lists available at ScienceDirect

Biochimica et Biophysica Acta

journal homepage: www.elsevier.com/locate/bbabio

Review

# Water in Photosystem II: Structural, functional and mechanistic considerations

Katrin Linke, Felix M. Ho *

*Photochemistry & Molecular Science, Department of Chemistry – Ångström Laboratory, Uppsala University, Box 523, 751 20 Uppsala, Sweden*

ARTICLE INFO

*Article history:*
Received 26 June 2013
Received in revised form 8 August 2013
Accepted 13 August 2013
Available online 23 August 2013

*Keywords:*
Photosystem II
Water
Channel
Proton
Oxygen
Grotthuss

ABSTRACT

Water is clearly important for the functioning of Photosystem II (PSII). Apart from being the very substrate that needs to be transported in this water oxidation enzyme, water is also vital for the transport of protons to and from the catalytic center as well as other important co-factors and key residues in the enzyme. The latest crystal structural data of PSII have enabled detailed analyses of the location and possible function of water molecules in the enzyme. Significant progress has also been made recently in the investigation of channels and pathways through the protein complex. Through these studies, the mechanistic significance of water for PSII is becoming increasingly clear. An overview and discussion of key aspects of the current research on water in PSII is presented here. The role of water in three other systems (aquaporin, bacteriorhodopsin and cytochrome P450) is also outlined to illustrate further points concerning the central significance that water can have, and potential applications of these ideas for continued research on PSII. It is advocated that water be seen as an integral part of the protein and far from a mere solvent.



## 1. Introduction

PSII is a large homodimeric transmembrane protein complex found in the thylakoid membranes of higher plants, cyanobacteria and green algae. At a recent count it consists of more than 40 protein subunits that are stably or transiently bound in the complex [1]. Its function as a water-plastoquinone oxidoreductase has been studied for many years, and readers are referred to the numerous excellent books and reviews for details of specific aspects of the biochemistry, mechanism and energetics of this enzyme [2–8]. Briefly, PSII utilizes the sun's energy to split water into electrons, protons and oxygen ($2\ H_2O \rightarrow 4\ e^- + 4\ H^+ + O_2$). Energy from absorbed photons is transferred from large chlorophyll antennae to the reaction center, where a special assembly of two chlorophyll molecules, known as $P_{680}$, is found. Excitation of $P_{680}$ leads to charge separation, where an electron is transferred to a pheophytin, the plastoquinone $Q_A$ and finally to plastoquinone $Q_B$. In the course of two charge separation events, $Q_B$ is reduced and protonated twice to give the plastoquinol $Q_BH_2$ that leaves the acceptor side of PSII, to be replaced by a plastoquinone molecule from the plastoquinone pool of the thylakoid membrane. The electron hole at $P_{680}^+$ is filled via a proton-coupled electron transfer reaction from a redox-active tyrosine residue, D1-Y161, also known as $Tyr_Z$. The $Tyr_Z^{\bullet}$ radical thus formed is re-reduced by a $Mn_4CaO_5$ cluster. This cluster is the catalytic heart of PSII, buried in the protein matrix on the luminal side of PSII. It is ligated by amino acid residues mainly from the D1 subunit of PSII, and is where water oxidation takes place. Four charge separation events lead to the accumulation of sufficient oxidation equivalents in the $Mn_4CaO_5$ cluster to oxidize two water molecules. During this process, the $Mn_4CaO_5$ cluster undergoes transitions between a number of intermediate states known as $S_n$-states ($n = 0–4$). These transitions are known collectively as the S-cycle. Overall, water oxidation is one of the most energetically demanding reactions in nature ($\Delta E_m = 1.23$ V), with the excited $P_{680}^*$ that drives the numerous steps in charge separation lying 1.83 eV above the $P_{680}$ ground state.

Water is much more than a solvent for PSII — it is also the substrate. In order for water to access the catalytic $Mn_4CaO_5$ cluster, channels are needed. Not only that, there is also the need to conduct protons away from the $Mn_4CaO_5$ cluster during the catalytic cycle as part of a process referred to as redox leveling [6,9,10] (see more details later). Water is involved by forming the pathways for this and other proton conduction events in PSII. As such, there is much interest in discovering both channels that permit the flow of substrate and products to and from the $Mn_4CaO_5$ cluster, as well as proton pathways that in other cases also involve water molecules.

*Abbreviations:* AQP, aquaporin; bR, bacteriorhodopsin; BRC, bacterial reaction center; CYP, cytochrome P450; FTIR, Fourier transform infrared; KIE, kinetic isotope effect; LCS, large channel system; MD, molecular dynamics; MSMD, multiple steered molecular dynamics; $P_{680}$, the primary donor in Photosystem II; PBD, photothermal beam deflection; PSII, Photosystem II; $Q_A$, the first quinone acceptor in Photosystem II/bacterial reaction center; $Q_B$, the second quinone acceptor in Photosystem II/bacterial reaction center; $Tyr_D$, the D2-Tyr160 residue in Photosystem II; $Tyr_Z$, the D1-Tyr161 residue in Photosystem II; WT, wild-type

* Corresponding author. Tel.: +46 18 471 6579.
*E-mail address:* Felix.Ho@kemi.uu.se (F.M. Ho).

0005-2728/$ – see front matter © 2013 Elsevier B.V. All rights reserved.
http://dx.doi.org/10.1016/j.bbabio.2013.08.003

In the following we give an overview of the advances in discovering the location, function and role of water molecules in PSII, including the channels and pathways associated with them. Beginning with an analysis of the position of the water molecules resolved in the highest resolution crystal structure to date, we will present a review of studies dealing with the structure and characterization of channels and pathways in PSII, as well as the mechanistic implications of their properties. As will be discussed below, water plays key roles in redox reactions both at and away from the site of water oxidation. Understanding the location, organization and role of water is an important part of unraveling the mechanism and function of PSII. Finally, we will extend our attention to a number of other well-investigated protein systems where water plays functionally important roles, demonstrating the importance of considering water as an integral part of the machinery of many protein systems.

## 2. Analysis of water molecules resolved in the PSII crystal structure

One of the major advances that came with the 1.9 Å crystal structure of PSII from *Thermosynechococcus vulcanus* (PDB ID: 3ARC, [11]) compared to earlier structures [12–14] is that for the first time a large number of water molecules were resolved. In total 2795 water molecules were found in the dimeric PSII complex. In this section, the distribution and location of these water molecules are discussed.

Visualization of the water molecules associated with the PSII complex with the protein and co-factors hidden shows that the majority of water molecules are found above and below the thylakoid membrane plane (Fig. 1A). Not surprisingly there are only very few water molecules found within the transmembrane region. While this is perfectly reasonable given that the transmembrane region is embedded in the hydrophobic region of the thylakoid membrane under physiological conditions, it is nevertheless an important observation to point out. PSII is not replete with water throughout its structure, and clearly not a uniform "sponge". For instance, no channels linking the $Mn_5CaO_5$ cluster to the stroma have been found in previous analyses of the structure [15,16] and this is confirmed by this crystal structure.

The constituent monomers in the PSII complex were individually refined in the asymmetric unit cell for building the crystal structure [11]. When the monomers and their associated co-factors and water molecules are overlaid onto each other, it can be seen that the protein structures are essentially identical. Analysis of the resolved water molecules reveals, however, that they are unevenly distributed between the two monomers, with 1457 water molecules being associated with one monomer, and 1338 water molecules with the other. The positions of the water molecules have been compared (Fig. 1).

Where two water molecules (or more strictly speaking, oxygen atoms assigned to water molecules) from the two monomers are located within a distance of 1 Å of each other, these were designated as conserved and overlapping water molecules. The remaining water molecules were designated as non-conserved water molecules between the two monomers. This analysis revealed that 294 (20%) and 175 (13%) of the water molecules from the two respective monomers (hereinafter referred to as monomer 1 and monomer 2) do not overlap with a corresponding water molecule in the other monomer (Fig. 1B). The remaining 1163 water molecules in each monomer are conserved between the two monomers.

Two comments can be made about this observation. Firstly, the majority of resolved water molecules in PSII are localized in well-conserved positions between both monomers. An average of 83% of the water molecules associated with each monomer are located at essentially exactly the same spots in both monomers. This suggests that these water molecules are stably coordinated in well-defined locations, therefore crystallizing well in the structure. These may therefore include important water molecules that could have a functional role or take part in reactions. Examples include the water molecules ligated directly to the $Mn_4CaO_5$ cluster, as well as chains of water molecules that may be involved in proton transport (discussed further below). It should be pointed out, however, that even mobile water molecules can have functional roles [17–19] and these may not be visible in the crystal structure. Also, the fact that water crystallizes in well-defined locations does not necessarily indicate a functional role. Nevertheless, water molecules found in locations conserved between the PSII monomers are unlikely to be there adventitiously.

Secondly, it is interesting to note that a significant number of water molecules (469 in total) are not conserved between the monomers (Fig. 1B). This represents an average of 17% of water molecules associated with each monomer that are not conserved. These are in some cases due to a slightly larger shift in position than the $\leq$1 Å search criteria employed (just over 40 water molecules would be reclassified as conserved if a criterion of $\leq$2 Å was used instead), but otherwise there are no corresponding water molecules in the monomers at these positions. These water molecules may represent sites that are not occupied as stably or consistently.

A further interesting analysis concerning the water molecules, conserved between the monomers or not, is whether they are located on the surface or in the interior of the complex. Since the complex is

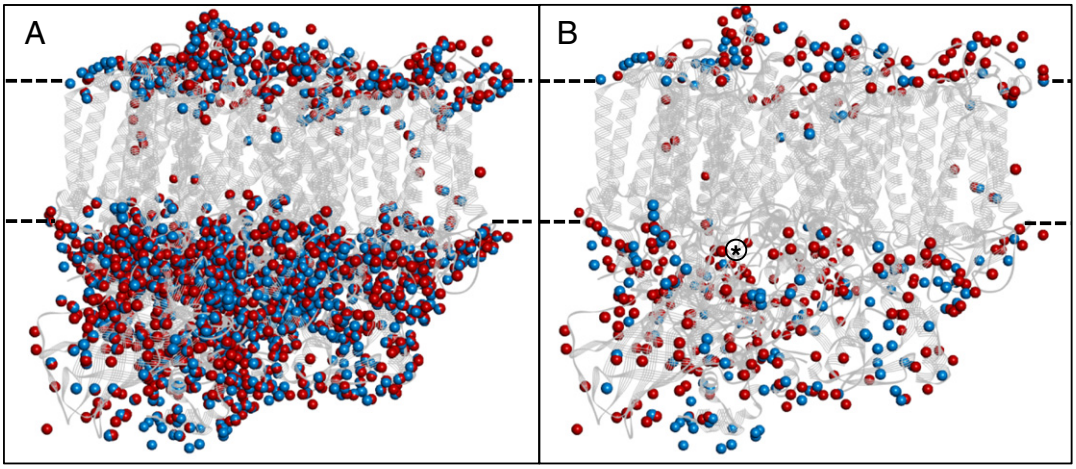


**Fig. 1.** Water molecules in the crystal structure of the monomers in the PSII dimer complex, overlaid onto each other. (A) All resolved waters molecules are shown (red: monomer 1; blue: monomer 2). (B) Only the water molecules not in found in corresponding positions in both monomers are shown. The protein structure of PSII is shown as a gray line ribbon. The dashed lines represent the membrane planes of the thylakoid membrane. To aid orientation, the location of the $Mn_4CaO_5$ cluster is marked with an asterisk.

found in an aqueous environment, it would not be surprising that water would bind to hydrophilic sites on the protein surface. Such surface water molecules, however, are arguably of lesser mechanistic interest, and more related to contact with the bulk solvent.

To investigate this more closely, the following analysis was performed on monomer 1. A solvent accessibility surface was calculated for the PSII monomer using a 1.4 Å probe criterion (Discovery Studio 3.1, Accelry Software Inc.). Water molecules that were found on this surface were then manually selected and designated as surface water molecules. The remaining water molecules were thereby internal water molecules (Fig. 2).

This analysis showed that 912 water molecules in monomer 1 (63%) could be defined as surface water molecules on PSII (Fig. 2A). Of these, 22% were found on the stromal surface, with the remaining 78% found on the luminal surface. This discrepancy likely reflects the larger surface area of the PSII complex exposed to the lumen compared to the stroma. Another factor may be the fact that the large phycobilisome antenna complex is attached to the stromal side of cyanobacterial PSII dimeric complex *in vivo*. The exact details of the attachment are still under investigation [20,21], but perhaps the stromal surface is more optimized for association with the antenna complex rather than to water molecules.

Of the remaining 545 internal water molecules (Fig. 2B), the majority of them (84%) are found on the luminal side of PSII among the extrinsic proteins PsbO, PsbV and PsbU and the substantial loops of the D1, D2, CP43 and CP47 subunits that extend from the transmembrane region below the luminal plane. The high number of water molecules here reflects the abundance of hydrophilic side chains in the extrinsic subunits, as well as a relatively open protein packing in this region which allows the entry of water molecules. This can be contrasted with the stromal side, where the surface is made up of the short loops linking the (hydrophobic) transmembrane helices, with little opportunity for water penetration. Some water molecules are nevertheless observed here, including the region around $Q_B$ (see below), as well as in association with chlorophyll molecules. In fact, as noted in [11] there are seven chlorophyll molecules where water serves as one of the ligands to the central Mg atom. These include the accessory chlorophyll molecules $Chl_{D1}$ and $Chl_{D2}$ that are closely associated with the $P_{680}$ complex, as well as two chlorophyll molecules (Chl-18 and Chl-31) that are found near and symmetrically placed about $P_{680}$.

The two analyses above (conserved *vs.* non-conserved between monomers; surface *vs.* internal water molecules) can be combined to reveal that essentially all of the water molecules not conserved between residues were surface-exposed water molecules. Of the 545 internal water molecules, only 21 were found to be non-conserved between the monomers. These include a number of molecules that lie in crevices open enough to be almost counted as surface accessible. Therefore, a large majority of internal water molecules are found in the same positions in both monomers, which is consistent with (though not necessarily prove) that they may serve either structural or functional purposes. Amongst these are chains of water molecules in channel structures that may indicate function associated with catalysis (discussed further below).

By contrast, a much higher proportion of the surface water molecules were not conserved between the two monomers. Of the 294 non-conserved water molecules, 273 were found on the surface. This represents 30% of the total number of surface water molecules, and reinforces the notion that the surface bound water molecules may be of little interest for the function of PSII. It is also worth noting that the average B-value for the conserved luminal internal water molecules in the crystal structure is 28 $Å^2$, compared to the much higher average B-factor of 51 $Å^2$ for non-conserved water molecules overall in PSII (PDB ID: 3ARC). In other words, the non-conserved water molecules show on average much higher isotropic displacements in the diffraction data (for comparison, conserved luminal water molecules that were instead found on the protein surface had on average an intermediate B-value of 41 $Å^2$).

In summary, the latest 1.9 Å resolution crystal structure of PSII has revealed that a large number of water molecules are associated with the protein complex. However, the distribution of water molecules is far from uniform throughout the protein matrix, with more than half of these molecules located on the protein surface and likely to be of lesser interest for PSII function. The transmembrane region is essentially free of water, but there are a number of interesting exceptions including ligation to chlorophyll molecules' central Mg. Nevertheless, it is clear that the luminal side of PSII with the extrinsic protein complexes is by contrast well-supplied with water. The fact that the water molecules found inside the protein matrix are in conserved positions in both constituent monomers also suggests that they are not adventitious. They allow us to verify earlier results on channel systems and bottlenecks (see below) and provide a platform for more detailed future analyses. Whether these are simply favorable hydrophilic pockets that happen to be water-filled or whether they have a functional roles clearly require further consideration and experiments. A number of these topics are reviewed and discussed below.

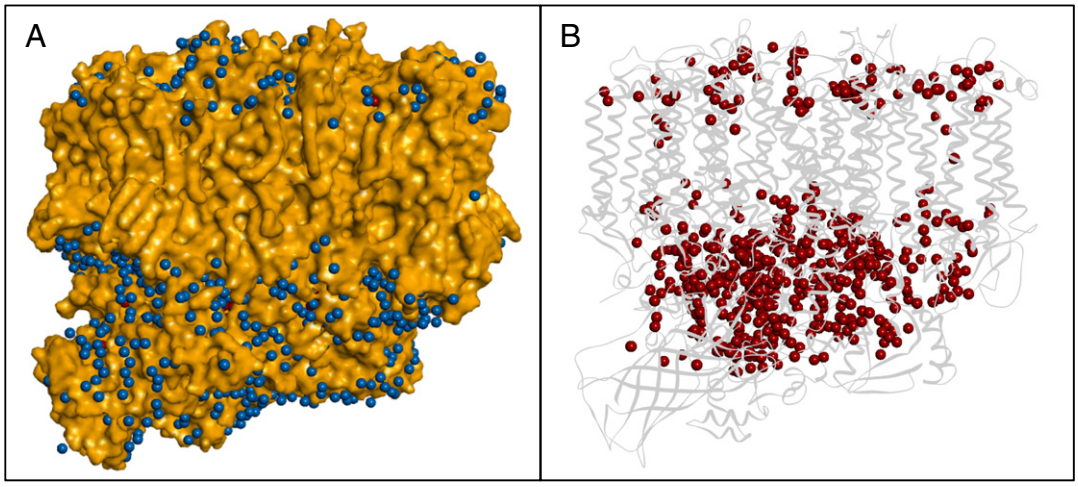


**Fig. 2.** Distribution of water molecules (A) on the surface (blue spheres) and (B) in the interior (red spheres) of PSII. The surface-bound water molecules have been removed from panel B for clarity. The protein structure of PSII is shown as a gray ribbon.

## 3. Photosystem II and the need for channels

Considering that the catalytic heart, the $Mn_4CaO_5$ cluster, is buried in the luminal side of the thylakoid membrane, molecular access would be limited, thereby restricting substrate and product diffusion in and out of the complex. Even before the availability of crystal structure data it had been suggested that entry and exit routes for substrate and products may be necessary for PSII to function efficiently, and that there may be control mechanisms involved ([22,23], reviewed in [15]). In the case of substrate water, it has been suggested that an over-abundance may cause undesirable side-reactions e.g. due to short circuiting of the water oxidation mechanism [22,24]. In the case of product $O_2$, highly reactive singlet $O_2$ ($^1O_2$) could be generated if ordinary triplet $O_2$ were to come into contact with triplet $P_{680}$ that can sometimes form as a result of recombination with $Pheo^-$ after initial charge separation ($P_{680}^+$–$Pheo^- \rightarrow {}^3P_{680}$ Pheo). As a powerful oxidant, $^1O_2$ can damage the protein structure or the $Mn_4CaO_5$ cluster, leading to irreversible loss of enzyme activity. For this reasons it was suggested that it is crucial that oxygen be removed quickly and reliably from the $Mn_4CaO_5$ cluster to minimize the chance of $^1O_2$ formation, and that specific channels may exist for $O_2$ transport in order to protect PSII [23,25]. Finally, as mentioned above, the removal of protons is as crucially important for PSII activity as charge separation and electron transfer due to the need for so-called redox leveling [6,9,26]. This is necessary to allow the same $Tyr_Z^{\bullet}$ with a constant redox potential to repeatedly reduce an increasingly oxidized $Mn_4CaO_5$ cluster by preventing accumulation of positive charge and thereby untenably high redox potentials (reviewed in [6]). Efficient and synchronized proton removal from the $Mn_4CaO_5$ cluster during water oxidation is therefore very important. Malfunction of proton egress will impair and even stop the reaction cycle and lead to energy loss or non-specific side reactions.

From all this evidence it becomes clear that certain protein infrastructure in PSII is essential for organized transport of substrate and products to and from the $Mn_4CaO_5$ cluster. Since the availability of crystal structure data for PSII a number of investigations have been dedicated to search for channels from the cluster to the surface of this large transmembrane protein complex. For water and oxygen movement, there is physical movement of the transported molecules, and therefore as a basic criterion the channels must be of a sufficient size and the nature of the amino acid residues lining the channels should be favorable, e.g. hydrophilic for water transport. Protons, in contrast, do not travel "naked" in an aqueous environment. Rather, net proton transport results from a series of proton transfer steps between hydrogen-bonded water molecules and/or protonatable amino acid side chains according to the Grotthuss mechanism [27–29]. This transfer takes place through the interconversion of covalent bonds and hydrogen bonds along a network of hydrogen-bonded water molecules and residues. Although net proton transfer is achieved, the proton that exits is not the same as the one that entered in the first place. (The proton is not a simple hydronium $H_3O^+$ either, but rather something in between the conformational extremes of an Eigen cation ($[(H_2O)_3H_3O]^+$) and a Zundel cation ($[H_2O-H^+-OH_2]$ [30,31]).

These requirements are not mutually exclusive, however, and assignment of channels or paths to the transport of a particular molecule(s) is a major challenge. For example, a water-filled channel could be used for water transport but potentially it can also function better as a proton pathway if the water molecules are well-ordered and hydrogen-bonded to allow efficient proton "hopping". The dynamics of hydrogen-bonded molecules would then be important for determining which is favored, since well-set hydrogen-bonded networks are preferable for efficient proton transfer. Gases can also permeate through water-containing channels, with the relative hydrophilicity/hydrophobicity of the gas and the channel affecting the rate [32–34]. Therefore it is relevant to ask whether channels are specialized for specific molecules or whether they can be used concurrently or consecutively for the transport of more than one species.

Previous reviews [16,35,36] have discussed in detail the development of proposals of channels in PSII. In the following, key features of these channels are summarized, though more focus is placed on recent developments since the publication of the 1.9 Å resolution crystal structure, as well as comparisons to earlier discussions. Readers are referred to the other reviews for more complete descriptions and analyses of the earlier studies.

## 4. Water and $O_2$ transport in PSII

### 4.1. Proposals based on static crystal structures

When research on channels in PSII first began, static models of PSII were analyzed for continuous spaces that extended all the way from the catalytic center to the lumen [15,37,38]. Channel radius was one of the main criteria investigated, since it determined which molecules would be able to pass through.

The channels described were named (i), (ii) and (iii) in Murray & Barber [37], "back", "narrow", "broad" and "large channel system" (LCS) in Ho & Styring [15] and channels A–G in Gabdulkhakov et al. [38]. A larger number of channels were identified in [38] due to the use of a smaller probe radius and allowance for short breakages which would nevertheless permit Grotthuss-type proton transfer via hydrogen bonding. With some minor differences, however, the three studies discovered mostly overlapping channel systems (compared in detail in [16], and correspondence tables for these different nomenclatures can be found in [16,36,39]).

On the basis of their structures and dimensions, each of the identified channels had the potential to transport water. At the same time, their suitability to transport $O_2$ or protons was also considered. The "back" channel in [15] correlates to channel (i) in [37] and channels A that forks into two different branches (A1/A2) in [38]. Channel (i) was suggested by the authors to serve as $O_2$ path while the other two studies assigned this channel to water transport. In [15] it was found that "back" channel was blocked right at the Ca of the $Mn_4CaO_5$ cluster, which restricted water access to the Mn ions. However, it was suggested that dynamic conformational changes at this point might allow passage to the "broad" channel and thereby the Mn ions.

Another strong candidate for a water-filled channel was the LCS described in [15], consisting of a number of branches radiating towards the lumen. Two branches of the LCS overlapped well with channel (ii) in [37] and channels B1/B2 in [38]. Considering the comparable large diameter of this channel it was proposed in [15,38] that its primary purpose may be efficient oxygen removal. As explained above, the presence of $O_2$ poses a significant threat to PSII, as it could react with excited triplet chlorophyll to form the highly reactive $^1O_2$. A voluminous escape route would prevent the accumulation of $O_2$ to high concentrations and avoid $O_2$ diffusion towards $P_{680}$.

A third channel system is the "narrow" channel [35], corresponding to channels D, E, F in [38] that lead into the "broad" channel [35], corresponding to channel (iii) in [37] and channel C and partially G in [38]. This system exits towards the PsbO and PsbU subunits and is a path that has generally been suggested to serve for proton transport. Reasoning for this assignment was its narrowness as well as its hydrophilicity, which would favor proton movement over water or oxygen transport. These channels also find agreement with other studies that have suggested residues D1–D61, E65 and D2–E312 (part of the "broad" channel and its equivalent) to be involved in a potential hydrogen-bonded proton path [12,40]. (Proton transport pathways will be discussed in more detail in a separate section below.)

Some experimental efforts have been made to identify potential $O_2$ channels in PSII using Kr- and Xe-perfusion studies on PSII crystals [14,38,41], but the results are so far inconclusive. As discussed in [16,36], only three of the 25 and 26 Xe-binding sites reported in [41,38], respectively, were in agreement ([14] was a precursor to [38], and only 10 sites were found there). Furthermore, the Xe-binding sites proposed

in [38] to constitute the $O_2$ exit pathway were located in the interface between the two PSII monomers in the dimeric complex, rather than within the transmembrane region of a monomer itself. As such, it is unclear whether these sites are physiologically relevant for $O_2$ removal from the $Mn_4CaO_5$ cluster. In any case, it is not certain that noble gas perfusion of crystals is optimal for identifying efficient $O_2$ exit pathways, as Xe-binding sites represent places where binding of such a hydrophobic species would be favorable enough to be resolvable in the X-ray diffraction data. This is arguably contrary to the aim of $O_2$ removal, where mobility should be high. Sites identified by perfusion studies may be more consistent with trapping sites (see [16] for further discussions and comparisons to other enzymes involving $O_2$ entry or exit).

### *4.2. Comparison of channel proposals with resolved water molecules in the crystal structure*

With so many well-resolved water molecules in the crystal structure, it becomes possible to compare them directly with the channel proposals. When the channels identified in [15] are overlaid onto the 1.9 Å resolution crystal structure it can be seen that the positions of the relevant water molecules are in excellent agreement with the channels (Fig. 3). This is despite the fact that the channels were calculated on the earlier 3.0 Å resolution crystal structure, confirming that there was already a high level of accuracy in the determination of the structure of the protein matrix there. This correspondence not only verifies the presence of these previously defined open spaces but also that they are favorable for the presence of water molecules. Even though they were originally not all proposed as water channels, it was nevertheless expected that they would contain water.

Although the water molecules in these channels correspond to only ~7% of all the resolved water molecules, we found that removal *in silico* of water molecules located in these channels leaves the $Mn_4CaO_5$ cluster in a much drier environment (Fig. 4). This is strong indication of the relevance of those channels for the water supply of the catalytic center of PSII. Of course, a much more important question is whether water would actually flow through these channels from the $Mn_4CaO_5$ cluster all the way to the surface. This is a question that has been addressed by more dynamic simulations (see below).

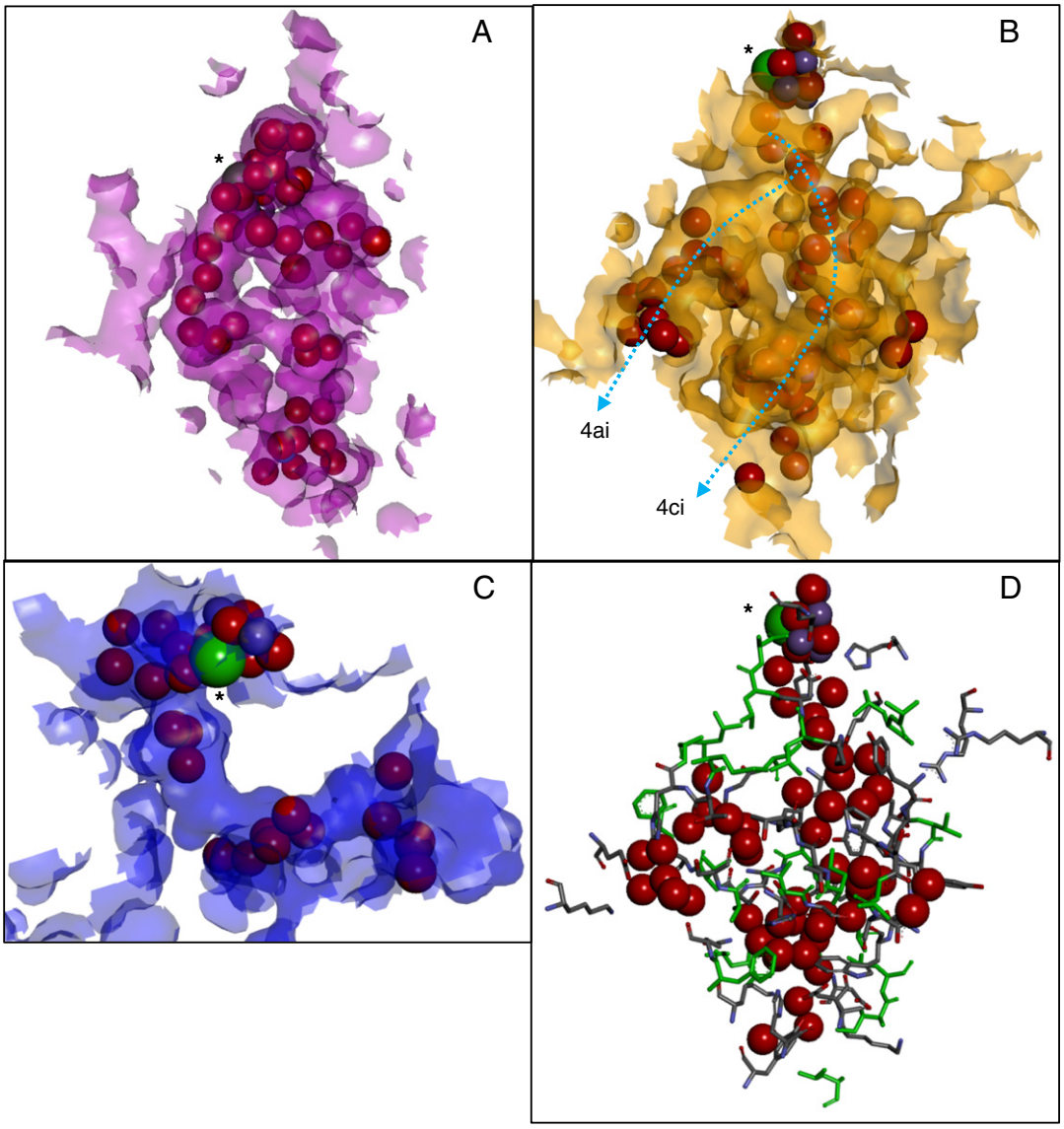


**Fig. 3.** Superposition of (A) the narrow and broad channels, (B) the large channel system and (C) the back channel [15] with water molecules in the same regions resolved in the 1.9 Å resolution crystal structure of PSII [11]. (D) The amino acid residues lining the large channel system are shown together with the resolved water molecules. Hydrophobic residues are colored green. In each panel, the position of the $Mn_4CaO_5$ cluster is marked with an asterisk. In (B), two of the oxygen channels identified in [42] (channels 4ai and 4ci) are marked with dashed arrows (see Section 4.2 for details).

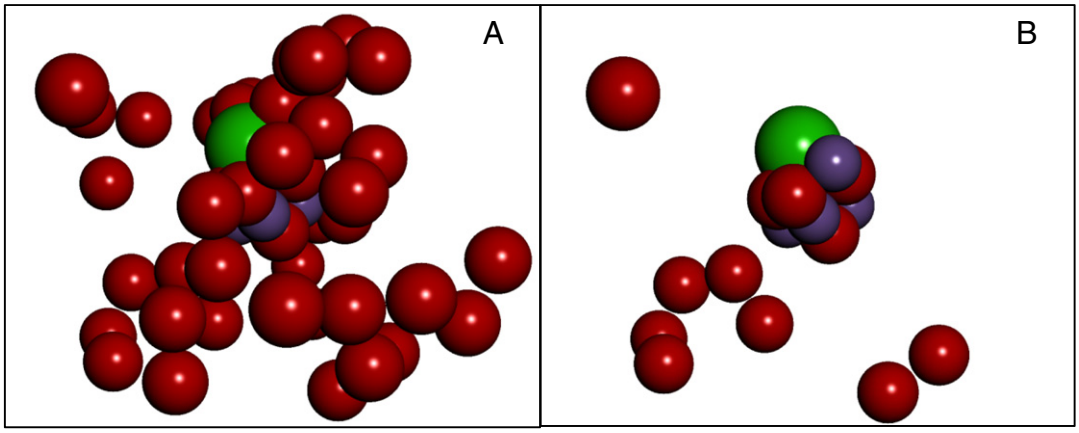


**Fig. 4.** Water molecules within a 10 Å radius around the $Mn_4CaO_5$ cluster. (A) All resolved water molecules in the region shown. (B) Water molecules located in previously identified channels removed.

An interesting observation can also be made here about the extent of water filling in the large channel system (LCS; Fig. 3B and D). While the LCS is in certain parts replete with close-lying, hydrogen-bonded water molecules, in other parts there are empty regions where no water molecules are resolved in the crystal structure. In Fig. 3D, the residues lining the LCS are visualized, with hydrophobic amino acid residues marked in green. Comparison of the gaps in water occupation in the LCS with these residues reveals that there is quite a good correlation between these gaps and hydrophobic residues, suggesting that either water molecules are not present at all or that they are too disordered to be resolved.

Not only is this correlation reasonable, it also provides further support for the proposal of the LCS being more favorable for $O_2$ exit. In addition to the larger volume of the LCS as mentioned above, these regions in the LCS with no resolved water molecules may be where $O_2$ diffuse through with reduced disruption to the hydrogen-bonding network between water molecules. This can be compared to the other narrower channels where $O_2$ molecules would have to displace and move past water molecules in single file in order to permeate (e.g. the much narrower "back" channel). Aside from the steric restrictions, this would also incur an energetic penalty in disrupting hydrogen bonds. A larger pool of water molecules as found in the LCS increases the chance for hydrogen bonds to reform should there be disruption due to the presence of $O_2$. Indeed, a very recent study [42] focusing particularly on the identification of $O_2$ diffusion paths in PSII using a combination of MD, implicit ligand sampling and wavefront propagation analysis has found three likely $O_2$ diffusion paths starting from the $Mn_4CaO_5$ cluster. Two of these correspond to two branches of the LCS (marked in Fig. 3B). It is particularly interesting to note that the most favorable $O_2$ pathway identified in [42] (Channel 4ai) overlaps with an arm of the LCS with an obvious gap in crystal water molecules (Fig. 3B & D), probably reflecting unfavorable binding for water, but not a problem for oxygen access. The other overlapping channel (Channel 4ci) was not identified as a water channel in [39], but it was found to be favorable for $O_2$ diffusion. This channel can be seen to overlap with the central branch of the LCS, and gaps can also be seen there.[1]

### 4.3. Proposals from simulations of the dynamic PSII

A significant limitation of the studies analyzing the crystal structure is that one static picture of the protein is considered. By contrast, it is known that even small changes in conformations under dynamic, physiological conditions can lead to temporary changes ("breathing") in the protein structure that cause changes in channel pore size, opening or closing of bottlenecks, or even formation of transient channel systems. Examples of this can be found in acetylcholine esterase [43,44], cholesterol oxidase [45] and 12/15-lipoxygenase [46]. More recent studies of PSII have therefore followed up on the earlier analyses of channels by applying methods taking into account protein dynamics and flexibility.

In Vassiliev et al. [47], molecular dynamics (MD) simulations were employed to study the movement of water through PSII and determine the most frequented water paths. A large number of paths were found and visualized using a fiber tracking technique to construct streamlines based on diffusional motion of all water molecules in the protein taken over the course of the entire simulation. These streamlines indicate regions where directional motions of water molecules are most pronounced, allowing the paths for water flow through the protein to be inferred, even if explicit water permeation was not observed in all channels due to the relatively short simulation times (when compared to the timescale for water diffusion). This fiber tracking technique is also used in e.g. medical magnetic resonance imaging (where it is known as diffusion tensor imaging [48,49]).

Using this technique, the majority of the earlier described channels were confirmed and refined, though new and additional pathways, connections and exit points were also discovered [47]. For example, more branches and outlets were found for the LCS (large channel system), which as a whole was shown to transport most of water molecules to the $Mn_4CaO_5$ cluster in this simulation. Under the dynamic conditions simulated, additional paths were found to connect the LCS to the "narrow" channel. On the other hand, at certain points of some water-filled channels (e.g. "back" channel), there were disrupted streamlines, suggesting disrupted water flow, possibly due to some other factors making water passage unfavorable (e.g. hydrophobicity). This illustrates that the dynamic MD approach provides insights beyond the spatial criterion used in the examination of the static crystal structures. Given the large number of water paths identified, Vassiliev et al. argued that water movement between the lumen and the $Mn_4CaO_5$ cluster is unlikely to be a problem. Nevertheless, some regulatory control may exist. The MD simulation revealed transient and rapid opening and closing in a number of paths and exits due to conformational changes of amino acid residues under dynamic conditions. This could have the effect of intermittently preventing water exit/entry and shows that there may be dynamic control mechanisms that limit/control water access.

This work has been recently extended to identify/verify water permeation paths using a water injection method to explicitly track the flow of water molecules, as well as for the first time consider the

[1] As the focus of that study was the diffusion of $O_2$ through PSII and not directly related to the current topic on the role and function of water in PSII, the reader is referred to [42] for further details of this important result.

energetics of moving water molecules through such channels [39]. Bruce and co-workers used a water injection method *in silico* based on the 1.9 Å crystal structure of PSII [11]. Starting from the PSII complex that was fully hydrated using a standard protocol, additional water was repeatedly injected at short intervals at the two water binding sites at the $Mn_4CaO_5$ cluster (W2 and W3 bound to the $Mn_4CaO_5$ cluster in [11]). This created a water over-pressure, driving the flow of water out of the complex. This was designed to accelerate water movement through PSII and overcome the issue of the short MD simulation times compared to the timescale of water flow through the complex. Water flow could then be explicitly followed rather than inferred from streamlines. Following the water movement thus observed, 21 water paths were identified. These paths were then assessed for viability for water permeation from an energetic point of view using multiple steered MD (MSMD) in which an external force was applied to water molecules to move them along the identified water paths. Potentials of mean force were calculated as a function of the position in pathways as individual water molecules were pulled through the channels from the bulk solvent towards the $Mn_4CaO_5$ cluster. This allowed the determination of the energies and activation barriers for water permeation through the different channels.

An activation energy threshold for water permeation of <15 kcal/mol filtered out all but five of the 21 channels initially identified by the injection protocol. While it was found that in general the barriers for water permeation in those five channels were low (<5 kcal/mol), indicating fast water movement in most sections, every channel contained at least one bottleneck region with an energy barrier of ~9–10 kcal/mol, indicating that water movement at these spots is slowed down. This suggested that unlimited water access to the $Mn_4CaO_5$ cluster does not exist. Using aquaporin as a benchmark, a water permeation rate of ~5000 $s^{-1}$ was estimated for the ~10 kcal/mol barriers found for these five channels. As pointed out in [39], this is a significant result. The energy barriers discovered support the idea of water flow and access regulation in PSII, but these permeation rates are still alone or in combination sufficient not to limit the rate of water oxidation (~50–100 turnovers $s^{-1}$: e.g. [50,51]).

Significantly, all five of the water channels overlap with earlier described paths, including channels that had been proposed for $O_2$ or $H^+$ transport. The "back" channel was however confirmed as not being permeable to water, with an energy barrier of ~22 kcal/mol in a hydrophobic area around residues CP43–F292, –F358 and D1–L91 (*c.f.* an estimated water permeation rate of ~$10^{-3}$ molecule $s^{-1}$ for a > 20 kcal/mol barrier: [39]). The possibility for $O_2$ transfer in one or more of these channels was however not excluded. There may also not be a unique path for water transport to the catalytic center, and the authors also noted that paths taken by the water molecules at the two separate binding sites at the $Mn_4CaO_5$ cluster in the first phase of the study did not cross each other [39].

Looking again at the overlay of the static channels and crystal water molecules (Fig. 3) and comparing this with the locations showing high energy barriers for water permeation [39], breakages in water chains in the crystal structure can indeed be seen at corresponding sites. For example, in the "narrow" channel [35] a gap in the water chain can be seen at D1–N338, D2–N350, CP43–P334 (Fig. 3A). This channel corresponds to channel 2 in [39] and at this point an energetic barrier to water permeation of 9 kcal/mol has been determined [39]. Thus the lack of a water molecule in the crystal structure is consistent with this position being less favorable for stable water coordination. Also, a significant break can also be seen at CP43–F292 and –F358 in the "back" channel, where despite a substantial channel radius there is no water molecule resolved here (Fig. 3C). Again correspondence can be found with the results in [39], where an energetic barrier of 22 kcal/mol was found at this point.

The positions of the crystal water molecules (or lack thereof) provide direct experimental confirmation of the theoretical calculations. The theoretical results in turn offer an explanation for the gaps observed in the water chains, suggesting that these were actual breaks due to unfavorable energetics, rather than being experimental artifacts. These studies also demonstrate that, although the initial analyses were performed on static structures, the structural details of the channels and their locations remain essentially valid even when protein dynamics and energetics are taken into account, as in the later MD studies. Such remarkable agreement between theoretical simulations/calculations and crystallographic structure data reinforces the potential and relevance of such computational methods in helping us to better understand the processes of molecule transport in PSII, among others.

## 5. Proton transport in PSII

### 5.1. Proton pathways to the lumen

As mentioned above, protons are generated during water oxidation, and for each charge separation event and concomitant oxidation of the $Mn_4CaO_5$ cluster, one proton needs to be removed from the cluster (though not necessarily during the same S-state transition) in order to achieve redox leveling [9,26,52]. Experimental investigations [53–55] have established that protons are released into the bulk aqueous phase during the S-cycle, with a pattern of (0,1,2,1) for the $S_1 \rightarrow S_2$, $S_2 \rightarrow S_3$, $S_3 \rightarrow [S_4] \rightarrow S_0$ and $S_0 \rightarrow S_1$ transitions, respectively. Additionally, although proton release is not uniform across the S-state transitions, it has been proposed that each deprotonation is in fact coupled to an oxidation of the $Mn_4CaO_5$ cluster in a strictly alternating manner to achieve redox-leveling (Fig. 5). The blockage of a proton transfer step would prevent the continuation of the catalytic cycle [10,26,52,56]. While this is experimentally most established for the $S_3 \rightarrow [S_4] \rightarrow S_0$ transition [57–59], the validity of this alternating pattern has been established though extension to other S-states through pH-dependence studies [60,61], time-resolved FTIR spectroscopy [62] and most recently the study of H/D kinetic isotope effects (KIE) during the S-state transitions using photothermal beam deflection (PBD) experiments [63] (Fig. 5). The role of electrostatic interactions around the $Mn_4CaO_5$ cluster in triggering proton release has also been investigated both in theory and experiment [58,59,64]. In addition to the need for redox leveling, since water oxidation by PSII contributes to the generation of a proton gradient across the thylakoid membrane that ultimately drives ATP synthesis by ATP-synthase, directional proton transfer against

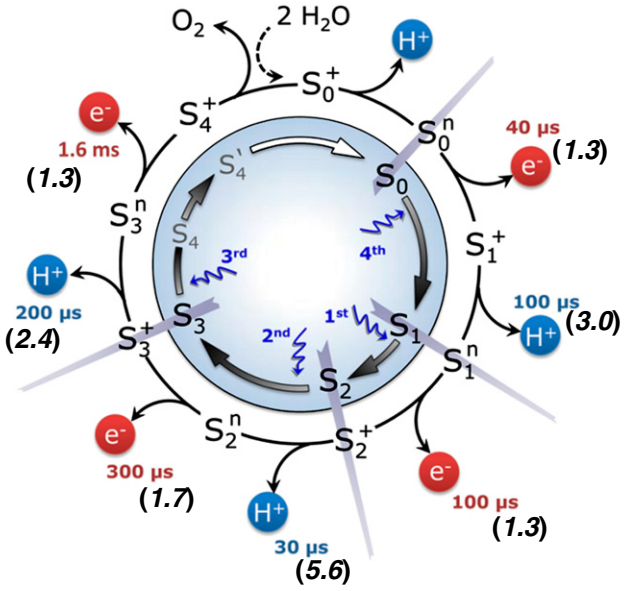


**Fig. 5.** The extended S-state cycle showing the time constants for the alternating electron and proton transfer steps. The KIE for each step are given in italics in parentheses. Adapted from [63], Copyright © 2012 National Academy of Sciences.

the proton gradient is required. Therefore, specialized pathway(s) supporting efficient Grotthuss-type proton transfer mechanisms have been proposed to exist in PSII [12,35,65–67]. Such pathways are expected to create local environments that direct proton movement and include mechanisms to prevent proton backflow back to the catalytic site. There is currently significant interest in identifying and characterizing putative proton pathways in PSII, and much yet remains to be understood.

In a range of experimental studies, impairment of PSII activity due to site-directed mutations has been assigned to disruption of a proton transport pathway (reviewed in [16,68]). Residues such as D1–D61, –E65 and CP43–R357 have particularly been implicated in proton transport. Building on these experimental studies and their 3.5 Å resolution crystal structure, Barber and co-workers proposed a potential proton pathway that leads all the way from D1–D61 near the $Mn_4CaO_5$ cluster to the extrinsic protein PsbO at the lumenal side of PSII [12,67]. In this proposal, residues such as D1–D61, –E65, D2–E312 and –K317 were also included. There were also early calculations of $pK_a$ values of amino acid residues near the $Mn_4CaO_5$ cluster that suggested possible paths for proton exit towards the lumen [40].

As mentioned above, Murray & Barber [37], Ho & Styring [15] and Gabdulkhakov et al. [38] have also proposed proton pathways based on their channel investigations. This function was suggested in [15] to be filled by the "narrow" and "broad" channel systems. These correspond to the channels D, E, F and channels C, G in [38], respectively, which were also proposed for proton transport. Murray and Barber proposed their water-filled channels (ii) and (iii) to be putative proton pathways (corresponding to branches of the LCS and the broad channel, respectively). As shown in the overlay analysis above (Fig. 3), these channels have been shown to be filled with water. However, consideration of the existence of water channels alone is not sufficient for assignment of proton transport pathways, given the requirement of directionality, efficiency and synchronization to the catalytic cycle. Recent research efforts have therefore directed away from water channels as the only target in favor of hydrogen-bonded networks of protonatable amino acid side chains in combination with well-ordered water molecules.

Two recent studies have focused on identifying hydrogen bonding networks in PSII with a view of identifying possible proton exit pathways and long-range connections within the protein complex. Service et al. [69] employed FTIR difference spectroscopy to look for hydrogen bonding networks conducive to proton conduction in wild-type (WT) PSII as well as the mutants D1–D61A, –E65A, –E329Q and D2–E312A. By examining changes in the $S_{n+1} - S_n$ difference spectra (were $S_n$ and $S_{n+1}$ represent the S-states n and n + 1, respectively) associated with these mutations, it could be seen that the properties of the $Mn_4CaO_5$ cluster were substantially altered. Substantial decreases in transition efficiencies in the $S_2 \rightarrow S_3$ and $S_3 \rightarrow S_0$ transitions were observed in these mutants, and remarkably even more so than mutations of some ligands to the $Mn_4CaO_5$ cluster (D1–D170H, –E189Q and –E342N).

Special focus was also placed on a characteristic negative band at 1747 $cm^{-1}$ that is associated with changes in the environment around a protonated carboxylate group. In the $S_2$–$S_1$ difference spectra, it could be seen that this band was eliminated by partial dehydration or the mutation of D1–E65A, –E329Q and D2–E312A. However, the D1–D61A mutation had no effect. These results were interpreted as indication that (1) an extended hydrogen bonding network connects D1–E65, –E329 and D2–E312 and an as yet unidentified carboxylate residue that is responsible for this negative 1747 $cm^{-1}$ band in the WT difference spectrum and (2) disruption of this network through mutation or dehydration stopped the transmission of structural perturbations that lead to changes around the carboxylate group responsible for this band, thereby eliminating this negative band. The fact that D1–D61A did not affect this band was interpreted as indication that the carboxylate group responsible for the negative band lies closer to the other three residues, even though D1–D61 can be seen in the PSII structure to be part of the same hydrogen bonding network as the other residues. Together with the data on impairments to S-state transitions, it was suggested that these residues may form a dominant proton exit pathway. The involvement of D1–E329 in proton exit is less clear, given that analysis of the PSII structure puts this significantly further away (~20 Å) from the other residues, and it remains open whether its connection in the extended network to the other residues are permanent or transitory. Also, it can be pointed out that since these residues are not all in direct hydrogen bonding contact with each other, water molecules are no doubt involved in any hydrogen bonding network. This can also be verified by examining the crystal structure.

In another study, Bondar & Dau [70] examined the distribution and pattern of charged and polar amino acid residues as well as bridging water molecules in the PSII complex on the basis of the 1.9 Å resolution crystal structure. Hydrogen-bonded networks resulting from these interactions were considered with regard to PSII functionality, in particular long-range proton transfer and conformational coupling between subunits. Clusters formed by carboxylic residues (Asp/Glu) were identified and numerous networks of different sizes, ranging from only two residues bound to one water molecule to bigger networks of carboxyl groups and water molecules were catalogued [70]. Several notable residues already implicated previously in proton transport (e.g. D1–D61, –E65, D2–E312) were included in these networks. It was suggested that many of the clusters could be connected together to form continuous hydrogen-bonding networks, potentially facilitating proton exit. Also, such connections may transmit information about protonation processes over long distances and trigger well-defined structural adjustments throughout the PSII complex. Potential effects of protein dynamics were also considered, with some potential links that were slightly too long for hydrogen bonding being possibly shortened transiently under physiological conditions or through specifically induced conformational changes directly linked to the catalytic cycle. The D1–D61/D2–E312 carboxylate dyad was particularly of interest, and it was suggested that it could share a proton and undergo protonation/deprotonation during the catalytic cycle. This may also be coupled to protein conformational changes due to extensive connections to other hydrogen bonding networks. Asp/Glu clusters and nearby water molecules on the luminal surface of the PSII complex were considered as possible "antennae" to facilitate proton release from the protein into the bulk. This possibility has also been suggested earlier by Shutova et al. [71] in relation to clusters of carboxylic acid groups on the surface of PsbO. Reduced oxygen evolution activity and retarded oxygen release kinetics observed in a PsbO-less mutant was attributed to a disruption to proton release from PSII [72].

We have also investigated a putative proton pathway in PSII through a parallel approach using both *in silico* MD simulations and *in vivo* site-directed mutagenesis in *Chlamydomonas reinhardtii* [73,74]. From MD simulations, a region at D1–D61, –E65, –N334, –R335 and D2–E312 has been identified as forming a "hotspot" with a highly interconnected hydrogen bonding network together with a number of water molecules (Fig. 6). In particular, D1–D61 was very stably connected to both D1–E65 and D2–E312 through chains of hydrogen-bonded water molecules, consistent with their putative role in proton transfer. To investigate the roles of the other residues, the mutants D1–R334K, –R334N and –N335R have been constructed both *in silico* and *in vivo*. Our *in vivo* results have shown impairment in photoautotrophic viability and oxygen evolution activity for the mutants, with activity in the order WT > R334K > R334N > N335R, and changes have also been found in the miss factor for the S-state cycle. These effects were reflected in the extent of disruptions to the hydrogen bonding network in the hotspot in a corresponding order, as seen in the MD simulations. It was found that the mutations of the D1–R334 and –N335 residues, though not protonatable residues that would directly participate in proton transfer in the WT PSII, nevertheless cause conformational changes that disrupt the integrity of

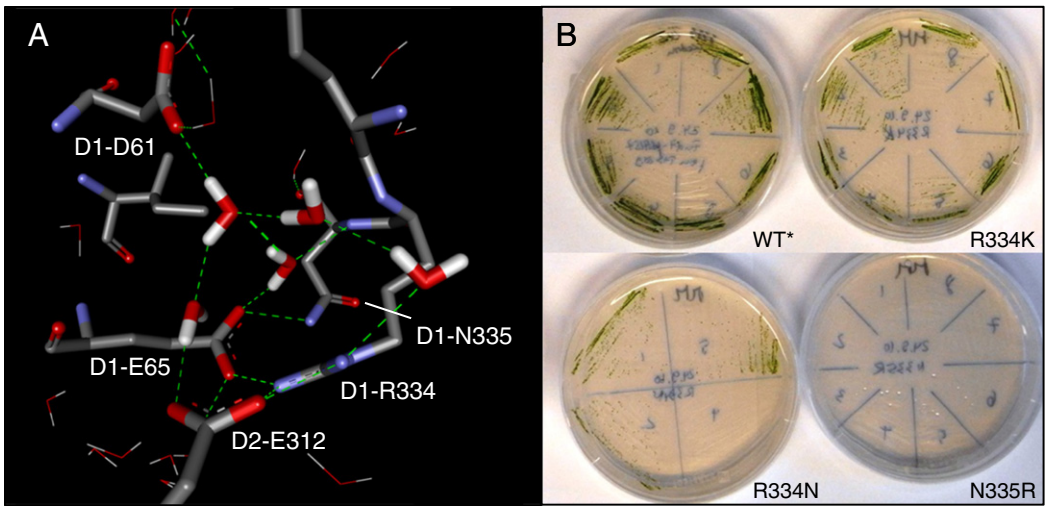


**Fig. 6.** Investigation of a putative hotspot for proton transport. (A) MD snapshot of the hotspot in WT PSII (B) *in vivo* photoautotrophic viability of WT* and mutants of *Chlamydomonas reinhardtii* grown on minimal medium.

the hotspot and reduce the connectivity via water molecules between D1–D61 and –E65/D2–E312, as well as the network of hydrogen bonds in the region more generally. This demonstrates the need to look beyond protonatable residues and consider the proton pathway as a whole, including the structural and electrostatic effects of other constituent residues in the pathway.

Our results also find agreement with the discussion in [70] on the possible role of D1–E65/D2–E312 dyad in proton transport and its connection to other hydrogen bonding networks as seen in the crystal structure. Considering the direct and stable salt-bridging interactions between D1–E65, –R334 and D2–E312, already evident in the crystal structure, we further suggest that this triad may represent a proton release group/proton loading site. Such sites have been proposed in e.g. bacteriorhodopsin [75,76] and cytochrome *c* oxidase [77]. It can also be noted the charged residues involved in the proton release group of bacteriorhodopsin are two Glu residues and an Arg residue, which is the same motif as observed here in PSII (Fig. 6A).

So far, the MD simulations have not explicitly accounted for the presence of a hydrated proton, and therefore transient effects of such changes in conformation and p$K_a$ are not yet accounted for. Such calculations would involve a higher level of theory and computation, but have been performed in other systems such as cytochrome *c* oxidase (e.g. [78]; see also more generally: [28,35,79]). Clearly there is scope for similar studies to be performed for PSII.

### 5.2. Proton conduction at the $Mn_4CaO_5$ cluster

Apart from identifying the overall path leading from the $Mn_4CaO_5$ cluster to the lumen, the question of the initial proton transfer steps directly at the cluster has also been of particular interest. As these steps are intimately coupled to the mechanism of the S-state cycle itself (including where and when individual protons are released from the $Mn_4CaO_5$ cluster), a strong dependence on the individual S-state transitions is expected. As the exact water oxidation mechanism is still under discussion (see for example reviews in [36,80–82]), it is not surprising that opinions differ in the literature in this regard. In all cases, however, water molecules bound to and in the second ligand sphere of the $Mn_4CaO_5$ cluster are proposed to play important roles in the transfer steps.

Prior to the 1.9 Å resolution crystal structure of PSII, Sproviero et al. [56,83] had considered proton release from water molecules bound to the $Mn_4CaO_5$ cluster for each of the S-state transitions, with CP43–R357 being assigned a special role in hydrogen bonding and proton removal. The involvement of non-substrate water at the cluster for proton transfer was described for the $S_4 \rightarrow S_0$ transition, where a water molecule between Mn(4) and D1–D61 was proposed to be the link between the $Mn_4CaO_5$ cluster and the proton exit pathway starting from D1–D61. A ligated, non-substrate water molecule at Mn(4) was also involved in the initial transfer steps after deprotonation of the substrate water.

In analyzing their 1.9 Å resolution crystal structure of PSII, Umena et al. [11] suggested that a group of water molecules close to the $Mn_4CaO_5$ cluster could be involved in a proton exit pathway leading from Mn(1)/Mn(4) to the lumen via a network that includes D1–Y161, –H190 and –N298 [11]. The direct involvement of D1–Y161 ($Tyr_Z$) in the removal of protons from the $Mn_4CaO_5$ cluster has been suggested before and is known as the hydrogen-atom abstraction model [84,85] (also known more generally as the hydrogen-atom transfer mechanism, or HAT mechanism, in the broader field of proton-coupled electron transfer reactions: [86,87]). However, experimental evidence [88] as well as energetics considerations (see e.g. discussion in [89]) have argued against this model. For the highly oxidizing potential required for water oxidation to be maintained at the powerful redox couple between $Tyr_Z$ and D1–H190 following charge separation, the proton must remain within this amino acid pair after tyrosine oxidation. Removal of proton to the lumen in connection to tyrosine oxidation would lead to a loss of this oxidation potential [89]. Therefore, it has been argued that an active proton exit pathway passing close to or directly involving $Tyr_Z$, as is the case for the suggestion in [11], is not likely to be favorable [90], since the proton from the $Tyr_Z$/D1–H190 couple could then also "slip" and exit to the lumen. Additionally, the proton path proposed in [11] passes through the residues D1–N298, –A411 and –N322 on the way to the lumen. Grotthuss-type proton transfer through such non-protonatable side chains or via their backbone moieties would be rather unusual. Indications of high energy barriers for proton transfer via this path have been noted in [90].

Based on cluster model hybrid DFT calculations, Siegbahn has proposed mechanisms for the transfer and release of protons from the $Mn_4CaO_5$ cluster during the $S_2 \rightarrow S_3$ and $S_3 \rightarrow S_4$ transitions [91]. The calculations included identification and structures of transition states between the S-states intermediates, thus revealing the proton transfer steps within the first and second coordination sphere water ligands around the cluster (Fig. 7). There were two particularly important second ligand sphere water molecules that were involved in both transitions, shuffling protons around the $Mn_4CaO_5$ cluster to transfer the released proton to D1–D61, the start of the proton exit pathway. One

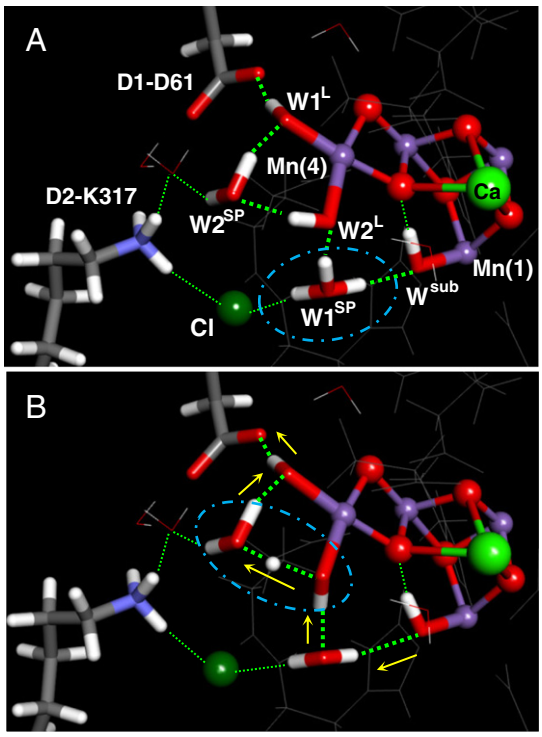


**Fig. 7.** Proton transport around the $Mn_4CaO_5$ cluster as proposed by Siegbahn on the basis of cluster model hybrid DFT calculations [91]. The (A) first and (B) second transition states from the $S_3^0$ state are shown. The $Mn_4CaO_5$ cluster and the chloride ion are shown as ball-and-stick models. The water molecules directly involved in proton transport are shown as stick models, as are the D1–D61 and D2–K317 residues. D1–D61 was proposed to be the first amino acid residue of the proton exit pathway. For clarity, the remaining amino acid residues and water molecules included in the calculations are shown as light line models. Key hydrogen bonds for the proton transport mechanism are shown as green dashed lines. The location of the proton and the water molecules involved are highlighted with the dashed ovals. The path for proton transport is indicated with arrows in (B). See the main text for the designations of the marked water molecules.
Adapted from and redrawn using molecular coordinates in [91]

of these second-sphere water molecules (labeled W1 in [91], but hereinafter referred to $W1^{SP}$ to avoid confusion in nomenclature) was found between a ligand water bound to Mn(4) (labeled W2 in the crystal structure [11], hereinafter $W2^L$) and the substrate water that was proposed to bind to Mn(1) upon the cluster reaching the $S_2$ state (hereinafter $W^{sub}$). $W1^{SP}$ was held in place by hydrogen bonding not only to both $W2^L$ and $W^{sub}$, but also to the chloride ion near the cluster in all but one transition states (a structural role for $Cl^-$ has also been recently been suggested in [92], where MD simulations showed that a salt-bridge formed between D2-K317 and D1-D61 upon $Cl^-$-depletion *in silico*, which could interfere with proton transfer). The other second sphere water molecule ($W2^{SP}$) was located between and hydrogen bonded to the ligand water molecules $W1^L$ and $W2^L$ bound to Mn(4) [11]. $W1^L$ is also hydrogen bonded to D1–D61 (Fig. 7).

In principle the same proton pathway around the cluster is used during both $S_2 \rightarrow S_3$ and $S_3 \rightarrow S_4$ transitions according to this mechanistic proposal. After $W1^L$ initially losing a proton directly to D1–D61, thereby forming the first transition state of the $S_2 \rightarrow S_3$ transition, proton transfers take place subsequently in the sequence $W^{sub} \rightarrow W1^{SP} \rightarrow W2^L \rightarrow W2^{SP} \rightarrow W1^L$ across the various transition states until $S_4$ is reached (Fig. 7). The distances and degrees of association between the protons with the water molecules vary between the transition states, but overall the same path is used to transfer protons from $W^{sub}$ to D1–D61 as $W^{sub}$ becomes increasingly deprotonated ahead of O–O bond formation. It can be seen from the transfer sequence that the second-sphere water molecules play a central role in proton transfer, alternating with the ligand water molecules. Another interesting result from this study is that the energy barrier for one of the proton transfer steps during the $S_3 \rightarrow S_4$ transition is almost as high as for O–O bond formation [91]. It was noted that the accuracy of the calculations was not high enough to definitively assign this step as rate-limiting, and the energy barrier for the $O_2$-release step has not yet been determined. Nevertheless, these are good indications for the importance of efficient proton transfer from the $Mn_4CaO_5$ cluster.

While Siegbahn has proposed a single proton exit pathway, multiple pathways have also been suggested. In addition to demonstrating the alternating pattern of electron and proton release during the S-cycle through the PBD and kinetic isotope effect (KIE) experiments, Klauss et al. [63] also proposed the existence of two distinct proton exit pathways at the $Mn_4CaO_5$ cluster.

One exit path is proposed to be used during the proton release associated with the $S_2 \rightarrow S_3$ transition. Here, the initial deprotonation/proton release is suggested to originate from a water molecule in the water cluster between $Tyr_Z$ and the $Mn_4CaO_5$ cluster as seen in the crystal structure. Distinct from other suggested proton paths, D1–D61 is not involved and this alternative exit path is found close to the $Tyr_Z$/D1–H190 couple instead (Fig. 8; questions regarding the hydrogen-atom abstraction mechanism are again likely to be relevant here). A large H/D KIE (5.7) and high activation energy (470 ± 50 meV) were observed for proton release step, which would in this model result in a delocalized proton vacancy in the water cluster. This proton vacancy is subsequently filled in the following electron transfer step during the overall $S_2 \rightarrow S_3$ transition. This electron transfer was proposed to be directly coupled in a concerted manner to a proton transfer from the $Mn_4CaO_5$ cluster (third step in Fig. 8). This concerted electron–proton transfer leading to the internal movement of a proton to the water cluster was suggested to explain the comparatively high H/D KIE of 1.7 for this otherwise electron-only transfer step in the extended S-cycle (Fig. 5).

In contrast to this proton pathway for the $S_2 \rightarrow S_3$ transition, a second proton pathway that does involve D1–D61 was proposed to be used during first deprotonation associated with the onwards transition from the $S_3$ state. In this step, a lower H/D KIE (2.4) and lower activation energy (180 meV) were experimentally determined. The proton exit pathway for the $S_0 \rightarrow S_1$ transition was not discussed in detail in [63], but intermediate values were observed both for the H/D KIE on the PBD transients (3.0) and the activation energy (340 ± 75 meV).

In proposing these two, S-state transition dependent pathways, Klauss et al. also relied on earlier studies of a D1–D61N mutant [93,94]. The $S_3 \rightarrow S_0$ transition was found to be significantly slowed down in this mutant, as measured by UV–Vis spectroscopy and polarographic measurements of $O_2$ release (~15–51 times slower in the D61N mutant compared to WT). The $S_2 \rightarrow S_3$ transition was, however, much less affected by the mutation (~2–4 times slower) and to a similar extent as for the $S_1 \rightarrow S_2$ transition that does not involve proton transfer (~2–5 times slower). Together with the PBD data, it was therefore argued that D1–D61 was involved in the proton exit pathway for the $S_3 \rightarrow S_0$ transition, but not for the $S_2 \rightarrow S_3$ transition. It is interesting to note that the possible existence of an alternative proton exit path was also raised in Dilbeck et al. [93] that was relied on by Klauss et al. In addition to the differences in $O_2$ release kinetics, there were also different H/D KIEs and pL sensitivities with respect to the miss factors for S-state transitions measured in the D1–D61N mutant compared to WT. An alternative proton pathway was therefore suggested to operate where the D1–D61N mutation was present. Note that this differs subtly from the proposal in Klauss et al. [63], where two separate proton pathways are used even in WT PSII, with the S-state transition in question being the decisive factor instead.

## 6. Oxidation of and proton transfer from $Tyr_D$

From the discussions above, the central role of water in proton transfer from and around the $Mn_4CaO_5$ cluster is evident. However, water is

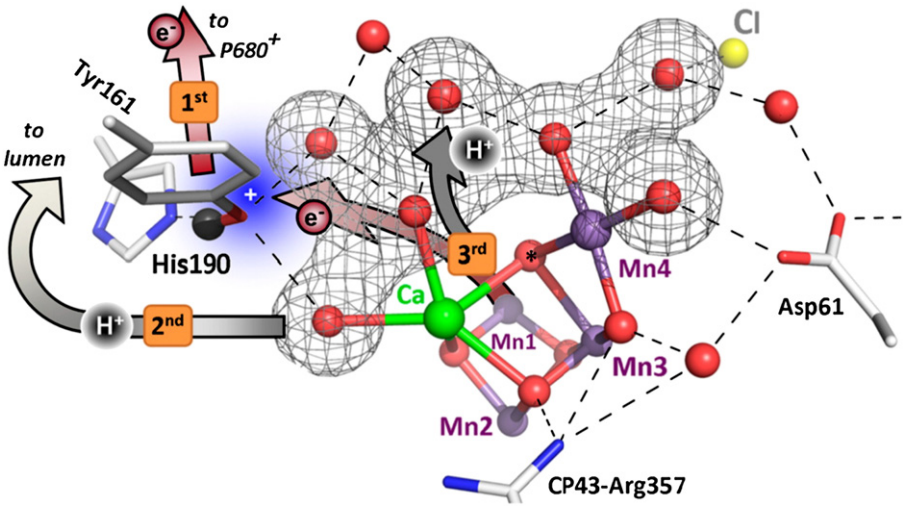


**Fig. 8.** Proton transfer sequence and pathway for the $S_2 \rightarrow S_3$ transition as proposed by Klauss et al. [63]. This path is distinct from the path involving Asp61 during the first proton release during advancement from the $S_3$ state (Copyright © 2012 National Academy of Sciences.).

also involved in reactions in other parts of PSII. One such reaction is the oxidation of the D2-Tyr160 residue, also known as $Tyr_D$.

$Tyr_D$ is located on the D2 subunit of PSII, symmetrically positioned with respect to $Tyr_Z$ on the D1 subunit. $Tyr_D$ can also be oxidized after light absorption by PSII, giving a long-lived radical. As for $Tyr_Z$, there is an adjacent His residue (D2-H189) within hydrogen bonding distance to $Tyr_D$, which has been implicated in this proton-coupled oxidation process [95,96]. Like $Tyr_Z$, the oxidation of $Tyr_D$ is also a proton-coupled electron transfer process, giving the neutral radical $Tyr_D^{\bullet}$. Unlike $Tyr_Z^{\bullet}$, however, $Tyr_D^{\bullet}$ has a much longer lifetime, and does not directly participate in the water oxidation mechanism. Certain possible roles in photoactivation, oxidation of overly reduced Mn-clusters and tuning of the charge separation process have however been proposed (see review in [97]). Also, in contrast to $Tyr_Z$ that is oxidized and re-reduced in the ns and μs–ms time ranges, respectively [98,99], formation of the $Tyr_D^{\bullet}$ takes place in the ms timescale, and involves a series of equilibria involving $P_{680}$, $Tyr_Z$ and the $Mn_4CaO_5$ cluster [100,101]. However, at elevated pH this oxidation is much more rapid and can proceed even at cryogenic temperatures [102,103]. Once formed, $Tyr_D^{\bullet}$ is generally stable for hours and can be easily detected by EPR spectroscopy. Further discussion and comparisons of $Tyr_Z$ and $Tyr_D$ can be found in [96,97].

The origins of the differences between $Tyr_Z$ and $Tyr_D$ oxidation was very recently investigated by Saito et al. [104]. The results of these studies have assigned special roles for nearby water molecules in affecting the energy profile of the mechanism of $Tyr_D$ oxidation.

In the 1.9 Å resolution crystal structure [11], a water molecule near $Tyr_D$ was found to occupy one of two alternative positions near the phenolic oxygen (proximal: 2.73 Å between the water and phenolic oxygen atoms; distal: 4.30 Å). The environment around $Tyr_D$ and these water sites is rather hydrophobic, with a number of Phe residues surrounding this water molecule. In addition to the disordered occupancies at these sites (occupancies of 0.30–0.35 and 0.60–0.65 for the proximal and distal sites, respectively: supplementary material in [11]), this indicates that there is significant water mobility in this region. Based on potential energy profiles obtained from QM/MM calculations, [104] reported that the proximal position could only be occupied where the $Tyr_D$ was in its reduced form ($Tyr_D$-OH), whereas the distal position was preferentially occupied where $Tyr_D$ has been oxidized to $Tyr_D^{\bullet}$ (Fig. 9A). Crucially, the phenolic proton in the $Tyr_D$-OH was found to be hydrogen-bonded to the water molecule in the proximal position rather than being hydrogen-bonded and shared between both the phenolic oxygen and Nε of D2–His189. It is instead the Nε of D2–His189 that remains protonated throughout and occupies this shared hydrogen bond position. This is a central difference with the $Tyr_Z$/D1–H190 situation, where it is the phenolic proton from $Tyr_Z$ that is shared between the two residues. The mechanistic consequence is that while the oxidation of $Tyr_D$ is also

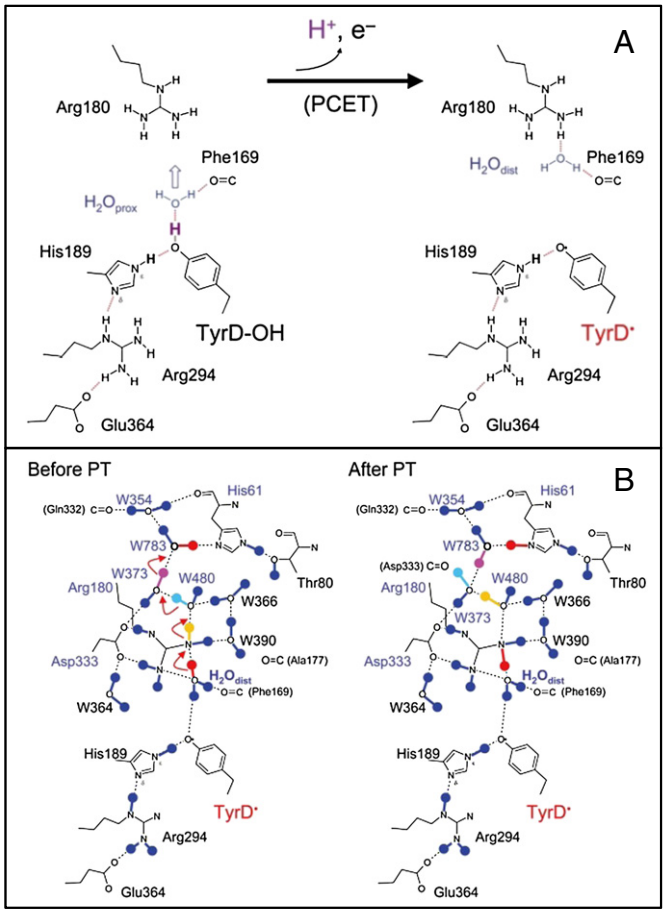


**Fig. 9.** Mechanism for the proton-coupled electron transfer during oxidation of $Tyr_D$ as proposed by Saito et al. [104] based on QM/MM calculations. (A) A water molecule moves between the proximal and distal positions as resolved in the crystal structure. (B) The concerted proton transfer along a chain of amino acid residues and water molecules away from $Tyr_D$ upon its oxidation.
Adapted from [104], Copyright © 2013 National Academy of Sciences.

a proton-couple electron transfer, the phenolic proton is not a "rocking proton" [105] in a low barrier hydrogen bond between the tyrosine and histidine residues upon tyrosine oxidation, as is the case for the oxidation of $Tyr_Z$ (reviewed in [96]). Rather, the proton from $Tyr_D$ it must be released elsewhere.

Upon $Tyr_D$ oxidation, therefore, it was necessary that (1) the phenolic proton of $Tyr_D$ be released away from the $Tyr_D$/D2–His189 region and (2) the nearby water molecule move from the proximal to the distal position at the same time (Fig. 9). Significantly, the proton transfer was energetically favorable according to the QM/MM calculations, with a fully concerted proton transfer reaction taking place over ~13 Å. Starting with a protonated water approaching the distal position adjacent to D2–Arg180, a concerted series of proton transfer reactions lead to proton transfer to D2–Arg180, through a chain of three water molecules, and ending at D2–His61 that is found near the luminal surface (Fig. 9B). The possibility of such a proton exit pathway was also raised by [11] (supplementary information). Interestingly, the participation of D2–Arg180, not usually a residue associated with proton transfer, was energetically possible here due to its salt-bridging to D2–Asp333, thereby forming a neutral ion pair.

The combination of the release of the phenolic proton into the bulk upon $Tyr_D$ oxidation and the requirement for the displacement of the water molecule near $Tyr_D$ in conjunction with this process was proposed as the reason for the long lifetime of $Tyr_D^{\bullet}$. The reverse processes required for re-reduction were energetically unfavorable. The reverse proton transfer would be an uphill process and the movement of the water near $Tyr_D$ back to the proximal position would incur reorganizational energy costs. Re-reduction was therefore proposed to be inhibited due to a lack of proton source and the absence of the connecting water at the proximal position [104].

In this proposal, therefore, the water molecules involved are directly linked to the oxidation mechanism and stability of the resulting $Tyr_D^{\bullet}$. Both the single water molecule near $Tyr_D$ and the water chain involved in proton transfer would have a one-way gating function that stabilizes the resulting $Tyr_D^{\bullet}$ radical. If this mechanism is correct, however, proposals concerning the electrostatic role of $Tyr_D^{\bullet}$ [97,102,106–109] become more questionable. In these earlier studies, the released phenolic proton was assumed to be localized near $Tyr_D^{\bullet}$, thereby acting as a positive charge in a hydrophobic environment influencing e.g. the location of the charge on $P_{680}$ after primary charge separation, the $pK_a$ of nearby ionizable amino acids and the redox potential of $P_{680}^{+}$. In [104], the proton is instead transported ~13 Å away from TyrD. Therefore, there would no longer be such charge localized at $Tyr_D$/D2–His189. Another point of consideration is whether the fully concerted proton transfer mechanism over ~13 Å proposed in [104] operates under dynamic conditions, given that the QM/MM calculations were restricted to a set chain of amino acid residues and water molecules that were energy optimized at each step of the calculation. A fully concerted mechanism would require a perfect alignment of all parts in the multi-component chain, as opposed to the more diffusive nature of the "traditional" Grotthuss mechanism, which may be more prevalent under dynamic conditions.

Finally, based on the possibility of an ancestral homodimeric origin for the D1 and D2 subunits of PSII, a comparison was made in [104] between the regions around $Tyr_D$ and $Tyr_Z$ as a way to identify a potential proton transfer pathway from the $Mn_4CaO_5$ cluster. This proposed pathway begins at $Tyr_Z$, and leads ultimately to D1–Asp61 through a number of water molecules ligated to the $Mn_4CaO_5$ cluster or the chloride ion/D1–Asn181. This is certainly an interesting analysis, but there are many open questions. With the path beginning at $Tyr_Z$, it is clearly reminiscent of the hydrogen-atom abstraction model, though it is not explicitly stated what the source of proton would be. The analogous path around the cluster does allow for $H^+$ shuffling, but no doubt the energetics around $Tyr_Z$ and $Tyr_D$ are very different due to the presence/absence of the cluster and the different protein environments. Note also that while D2–H61 lies near the luminal surface, D1–D61 is still fairly buried inside the protein due to the presence of the extrinsic subunits nearby, in particular PsbO. Therefore while an analogous path may be identified geometrically between the D1 and D2 subunits, caution is required before more experimental and/or computational evidence is available.

## 7. Proton pathways at $Q_B$

Apart from the donor side of PSII, water molecules/chains have also been proposed to be of importance on the acceptor side, in particular for the protonation of $Q_B$.

The plastoquinone $Q_B$ is the final electron acceptor in PSII, which upon accepting two electrons and concomitantly two protons to form plastoquinol $Q_BH_2$ exchanges with oxidized plastoquinones in the plastoquinone pool in the thylakoid memebrane. Electron transfer from $Q_A$ to $Q_B$ is mediated by a non-heme iron, which is coordinated by four histidine residues (D1–H215, –H272 and D2–H214, –H268) and a bidentate bicarbonate ligand (for a recent review see [110]). The steps in protonation are much better understood in the functionally analogous $Q_B$ of the bacterial reaction center (BRC) of photosynthetic bacteria, and have been used as a starting point for identifying pathways for $Q_B$ protonation in PSII (e.g. [111]; see also [110,112]). Two (partially overlapping) pathways are believed to be involved in the delivery of each of the two protons to $Q_B$ in BRC. Both start near the surface, ending with either Asp-L213 and Ser-L223, or Glu-L212 to protonated $Q_B^-$ and $Q_BH^-$, respectively, and water molecules have been shown to be part of these transfer pathways. It should be noted, however, that the details of this mechanism (e.g. the identity of the pathways, the sequence of electron and proton transfers and loading events, the protonation states of the amino acids involved during the cycle, the orientation and binding of $Q_B$) have not been uncontroversial [110,113–119].

Key residues near the $Q_B$ site of PSII (e.g. D1–His215, –E244, –Tyr246, –Tyr246, –His252, –Ser264) have been variously considered to transfer protons to $Q_B$, in hydrogen-bonded networks probably in conjunction with water (see for example: [110,112,120–122]). The residues D1-His252/Ser264 in PSII are analogous to Asp-L213/Ser-L223 in one of the proton pathways for in BRC. The PSII residues here are found close to the stromal surface and are in proximity of a number of resolved water molecules in the crystal structure. Therefore, there is likely to be easy access to protons from the bulk for protonating $Q_B$ via these residues [112]. However, there are also key differences between PSII and BRC around $Q_B$. Significantly, the important Glu-L212 residue in BRC is replaced by an alanine in the corresponding position. The most recent crystal structure of PSII [11] also shows a distinct lack of resolved water molecules near the $Q_B$ binding site. The bicarbonate ion ligating to the non-heme iron has also long been known to be unique to PSII.

Results from a very recent QM/MM study [123] have suggested that the first protonation of $Q_B$ after the first reduction indeed takes place via D1–His252 and –Ser264. For this first protonation of $Q_B$ in PSII, these amino acid residues appear to play the key roles, with involvement of water limited to bulk water molecules providing external protons, as also suggested in [112]. Mutants at D1–Ser264 have been shown to confer herbicide resistance by interfering with herbicide binding to the $Q_B$ pocket [124–129]. More importantly for the present discussion, however, these mutants nevertheless show impaired growth and PSII activity in the absence of herbicides. This would be consistent with reduction in $Q_B^-$ protonation efficiency, leading to a block on the PSII acceptor side. There is also indication that the $Q_B/Q_B^-$ potential is also affected [124,126].

A more intriguing aspect is the protonation of $Q_BH^-$, since the residue in the position homologous to Glu-L212 in BRC is alanine and thus unable to protonate. Here, water molecules have been proposed to play a more important mechanistic role.

It has been proposed [123] that the D1–His215 residue that is ligated to the non-heme iron provides this proton to $Q_BH^-$. It was argued that

the p$K_a$ of D1–His215 is lowered due to its ligation to the positively charged non-heme iron, thereby making proton donation from Nδ possible (Fig. 10A; ligation to the non-heme iron is via the Nε atom). Reprotonation of D1–His215 could then occur via the bicarbonate ion bound to the non-heme iron. Although the bicarbonate ion is connected to water molecules leading to the bulk, the distance between the bicarbonate ion and D1–His215 is too large for favorable direct $H^+$ transfer. However, an elongated electron density originating from the nearby D1–Tyr246 residue was observed in the crystal structure. It was suggested in [123] that this may be evidence for a tyrosine peroxide (Tyr-OOH) having been formed at this point, possibly due to a reaction between D1–Tyr246 and a water molecule, as an artifact of the X-ray radiation used for data collection. This water molecule would have been located between the bicarbonate and D1–His215. Its presence would then complete a hydrogen bonding network that could transfer protons from the bulk to D1–His215 via the bicarbonate ion and D1–Tyr246. According to this proposal, water molecules would play an important role both in conducting protons to the bicarbonate ion, as well as being a crucial bridge to the D1–His215 residue.

The involvement of bicarbonate and D1–His215 during the protonation of $Q_BH^-$ was also proposed earlier by Shevela et al. [112]. An important difference in that proposal compared to that in [123] is that the proton pathway from the bicarbonate ion to $Q_BH^-$ was suggested in Shevela et al. to go first via the Nε atom of His272, then the Nε atom of D1–His215 and finally the Nδ atom of D1–His215 before reaching $Q_BH^-$. Noting that the first two steps involve proton transfer via the ligating Nε atoms of D1–His272 and –His 215 that are bound to the non-heme iron, it is unclear whether this path is favorable.

Examining the region between $Q_B$ and the non-heme iron in the crystal structure, there is an empty site that is able to accommodate the extra water molecule proposed in [123]. An interesting additional observation that can be made here is that this pocket is rather hydrophobic (Fig. 10B). In addition to D1–His215, –His272 (ligands to the non-heme iron), –Ser268 and –Tyr246 (mentioned above), this pocket is lined by D1–Val219, –Ile248, –Ala251, Phe265 and –Leu271. Given the hydrophobicity of this space, a water molecule located here could exhibit high mobility. This would seem to be opposed to the requirement of a stable and well-ordered water chain for efficient proton transfer. But there may be a mechanistic reason behind this. Just as the water occupying the alternate positions in the hydrophobic region at $Tyr_D$ may have mechanistic significance ([104], see above), perhaps a water molecule fills this pocket only after the first reduction and protonation (via D1–His252 and –Ser264) of $Q_B$. The presence of this water molecule would thereby be mechanistically coupled to the need for a complete proton pathway for $Q_BH^-$ protonation. This would also link the site of $Q_BH^-$ protonation to the specific step in the $Q_B$ reduction mechanism. Water access to this pocket is hindered by a bottleneck formed by D1–Tyr246, –Ser268, –His272 and the bicarbonate ion, but dynamic movement possibly linked to the first reduction/protonation could allow water entry, perhaps triggered by the formation of the $Q_BH^-$ species that is formed after the second reduction step. Note that there are examples in others proteins where transient proton pathways are formed in synchrony with specific steps in the mechanism (e.g. bacteriorhodopsin, cytochrome P450; see below).

It can also be noted that the four water molecules that have been suggested to link the bicarbonate to bulk water [112] do not form a complete hydrogen-bonded chain, and two of these are not conserved between the two monomers according to the analysis above. However, this is probably a reflection of high mobility of water molecules near the bicarbonate ion. In fact, when the solvent accessibility surface calculated above (Fig. 2A) was more specifically examined in this region, it could be seen that these water molecules are located in a larger channel (Fig. 11). The empty spaces in this channel may be indicative of mobile water molecules. Furthermore, it was found there was another channel

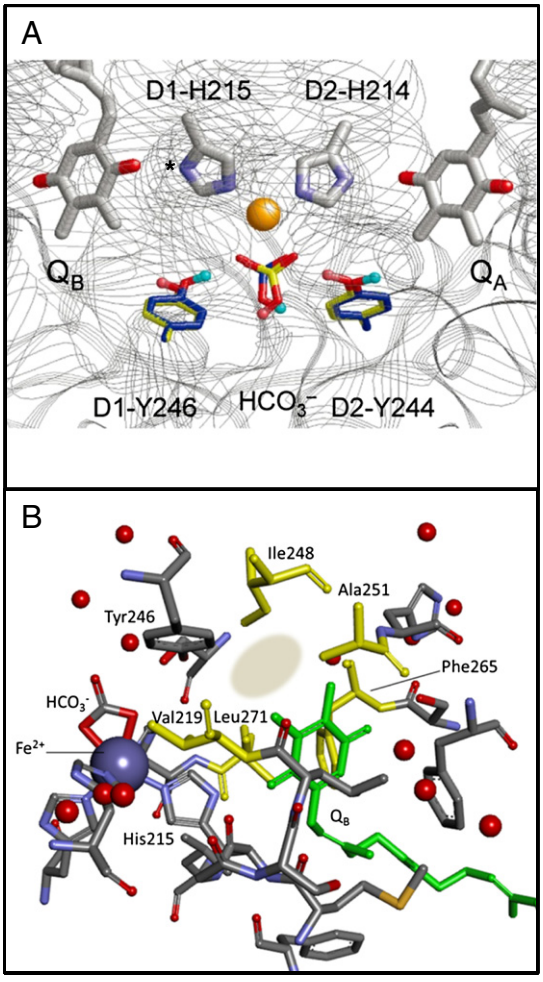


**Fig. 10.** Protonation of $Q_B$ in PSII. (A) Key residues and co-factors around $Q_B$ that may be involved in $Q_B$ protonation. Different conformations for the bicarbonate ion and tyrosine residues depending on the oxidation state of $Q_A$ and $Q_B$ are shown (see [123] for details). The Nδ atom of D1–His215 proposed in [123] to protonate $Q_BH^-$ is marked with an asterisk. (Adapted from [123], Copyright © 2013 National Academy of Sciences.) (B) Empty site (shaded oval) between $Q_B$ (green) and the non-heme Fe (purple sphere) on the acceptor side of PSII. The hydrophobic residues in the region are colored yellow. Water molecules resolved in the crystal structure are shown as red spheres.

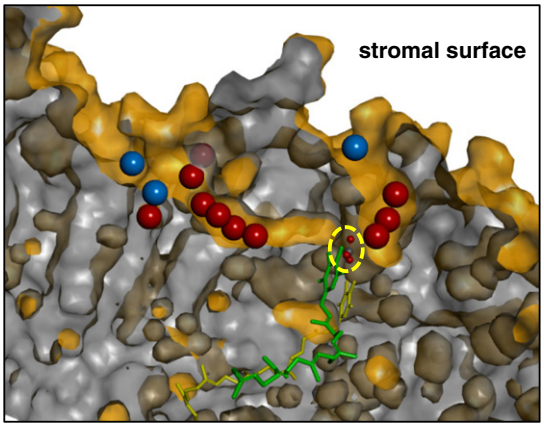


**Fig. 11.** Cross-sectional view of water channels leading to the bicarbonate ion (ball-and-stick representation; dashed oval) between $Q_A$ (yellow) and $Q_B$ (green) based on examination of the solvent accessibility surface (see Fig. 2 and accompanying text). Water molecules in the channels are shown as space-filling spheres (blue: surface exposed molecules; red: non-surface exposed molecules). The channel to the right contains the water molecules proposed in [112] to conduct protons to the bicarbonate ion.

that led to the bicarbonate ion. Although no water molecules in this channel were located immediately adjacent to the bicarbonate ion (Fig. 11), taken as a whole it is possible that there are again mobile water molecules in this channel that could access the ion. It is unclear how such mobility would affect the protonation reactions. It should also be remembered that phycobilsome is usually attached to the stromal side of PSII under physiological conditions. It is not yet known how water and proton access to and via these channels would be affected by this.

## 8. Water: a controlled and a controlling element

From the overview above, it can be seen that water in PSII is much more than just the solvent in which the enzyme is immersed. As the actual enzyme substrate, there may be mechanisms for controlling its access to the active site. The energy barriers found for water movement through channels [39] and the dynamic opening and closing of some channels [47] may be indications of this. These correlate also with gaps in water occupation in otherwise open channel structures as shown in the crystal structure ([11]; see analysis above). However, as conductors of protons, water molecules can serve another role as a *controlling* element that mechanistically couples proton transport to the catalytic cycle, facilitating efficient proton transport at specific stages of the cycle.

In this final section, a brief overview of some examples illustrating these different roles for water is given. It will be seen that the line between water being the controlled or the controlling element blurs, but these are nevertheless interesting perspectives to consider. The mechanisms through which these respective controls are achieved can be interesting for further study of processes involving water in PSII. Specific examples from three proteins are presented: aquaporins, bacteriorhodopsin and cytochrome P450.

### *8.1. Aquaporins — mechanisms for controlling water flow*

Aquaporins (AQP) form a big protein family and are well known for their high-speed water transport across biological membranes. The protein forms a transmembrane pore where water molecules flow through in single file. However, AQPs strictly exclude proton conduction despite the existence of a water chain, due to an electric field effect culminating in a large energy barrier at a conserved double arginine–proline–arginine (NPA) motif in the middle of the channel. Proton conduction is not actively prevented by water molecules. This research has been reviewed extensively and will not be discussed further here, but it is nevertheless a salutary reminder that just as the absence of a permanent water chain does not exclude proton conduction under dynamic conditions, the presence of a chain does not guarantee proton conduction either. The reader is referred to other reviews [28,34,130,131] for further details concerning the mechanism of proton exclusion in AQP. Instead, attention is drawn to mechanisms for gating water flow through APQ that have been proposed during recent years, as an example of water being the controlled element in a protein.

Gating mechanisms for water permeation have been suggested on the basis of X-ray crystallographic and MD studies. These share a theme of conformational changes that lead to opening and closing of the channel. For example, in AQPZ from *E. coli*, control of water flow has been proposed to be achieved by conformational changes of the arginine residue Arg189 that is part of the well-conserved aromatic/arginine selectivity filter that lies in the narrowest part of the pore [132–134]. The guanidino group of Arg189 has been found in two distinct conformations in the crystal structure of AQPZ, which were suggested to represent the open and closed states of AQPZ [133]. Subsequent MD simulations verified that the upward orientation of Arg189, where the guanidino groups is oriented parallel to the length of the channel, allows water flow while in the downward position the guanidino group forms a hydrogen bond with Tyr183, thereby closing the selectivity filter [134]. Furthermore, interaction of His174 with Arg189 appears to be important in controlling the position of the ladder [132] and removal of the long side chain of arginine in simulations of a Arg189Ser mutant resulted in a permanently open channel [134].

By contrast, a more dramatic conformational change has been suggested in the spinach AQP SoPIP2;1. Here, an external loop (D-loop) can flip towards the N-terminus across the channel opening to obscure the cytoplasmatic pore entrance, essentially functioning like a plug [135]. This closed conformation is thought to be stabilized by the interaction of the conserved residues Arg190 and Asp191 in the D-loop with the N-terminus of SoPIP2;1. Disruption of the hydrogen bonding interaction between the D-loop and the N-terminus through phorphorylation of certain serine residues has been suggested to trigger channel opening *in vivo* [135–138], whereas protonation of the conserved His193 (e.g. low pH) leads to stabilization of the closed conformation [135]. Gating by phosphorylation of serine residues has also been suggested for AQP4 in mammalian brain [139] and AQP2 in mammalian kidney [140].

### *8.2. Bacteriorhodopsin — making and breaking of water chains for controlling proton conduction*

As a controlling, rather than a controlled element, there are examples where the formation or breakage of a chain of water molecules has been attributed to the regulation of proton transport. These changes are generally triggered by changes in amino acids interacting with critical water molecules. In a sense the amino acids involved can be viewed as the transducing element that connects specific events in the functioning of the protein to the creation or disruption of a viable proton transport path provided by the water chains.

The detailed mechanism of the proton transfer mechanism of the light-driven proton pump bacteriorhodopsin (bR) has been extensively studied through a variety of biochemical, spectroscopic, crystallographic and computational studies. Of particular interest have been the steps following light absorption and photoisomerization of the retinal chromophore bound to Lys216 via a Schiff base, including the sequence and structural changes through the individual steps of the photocycle, as well as the network of amino acids residues and water molecules involved in the storage and transfer of protons. The literature is vast and mechanistic proposals as well as controversies abound. For more details, see a number of reviews and recent papers on the topic: [76,141–147]. Here, two examples of recent proposals involving the bR mechanism that are of particular relevance for the current discussion are presented.

The first concerns the uptake of proton from the cytoplasmic side of bR in the final stages of the photocycle, leading to reprotonation of the Schiff base (Fig. 12A). Based on time-resolved FTIR spectroscopy and MD studies it was recently proposed that a three-water chain transiently forms between Asp96 and Lys216 during the final reprotonation step [17]. While only two water molecules are resolved in this region in the crystal structure of ground-state bR, it was proposed that a third, mobile water molecule completes this chain as a result of conformational changes during the reprotonation step. The existence of a dynamic water chain between Asp96 and the Schiff base in this later phase of the photocycle was also observed in a more recent study based on both crystallographic analysis of a triple-mutant of bR as well as MD simulations [147]. In addition, the protonation state of Asp96 was found to be determinative of whether the cytoplasmic side of the bR channel was accessible to bulk water. Only when Asp96 was deprotonated was the channel open; conformation changes closed the channel whenever the Asp96 was already protonated. It was thus proposed that Asp96 acted as a "latch" for gating the flow of water (and therefore protons) from the cytoplasm to Asp96 [147]. Therefore, it can be seen that water acts as part of the controlling element for proton transfer here, whereby the changes associated with a particular step in the

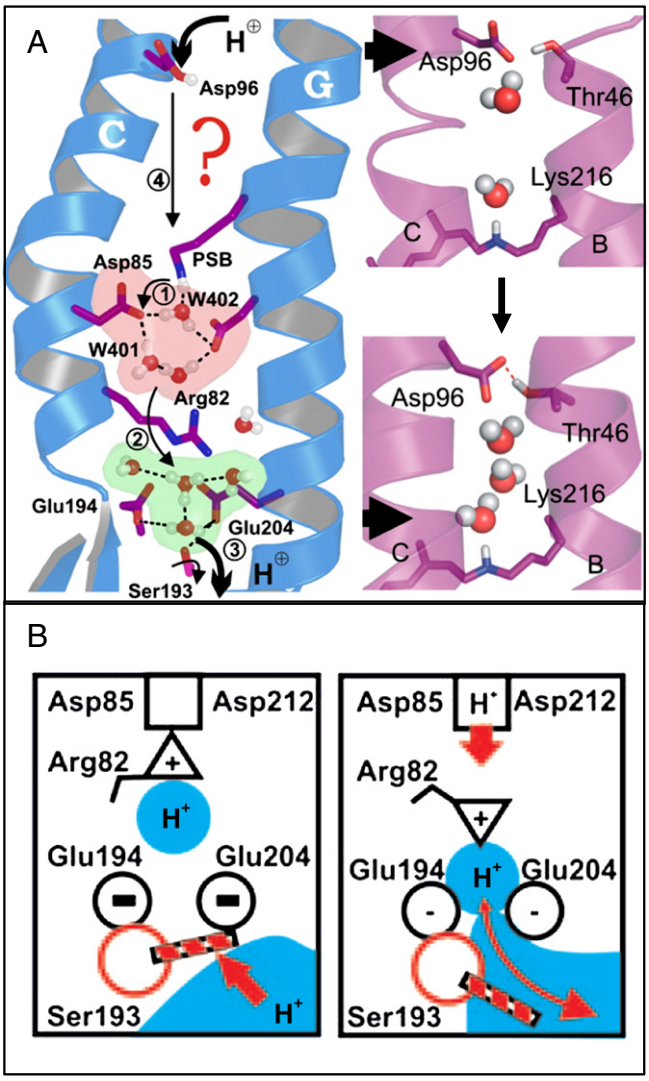


**Fig. 12.** Water-mediated proton uptake and exit in bR. (A) Proton uptake for reprotonation of the Schiff base in bR. A transient chain of three water molecules is proposed to form from an original two during the reprotonation phase of the photocycle. (Adapted from [17] Copyright © 2011 National Academy of Sciences.) (B) Proposed gating mechanism for unidirectional flow of protons from bR (Adapted from [148] © 2010 Wiley-VCH Verlag GmbH & Co. KGaA, Weinheim.).

photocycle is transduced by conformational changes in the protein that lead to the making or breaking of proton transport paths via water chains.

The second recent proposal concerning bR is on the proton release side and concerns the unidirectional nature of the proton transfer from bR (Fig. 12B; [144,148]). Through a combination of time-resolved FT-IR spectroscopic studies and MD simulations on WT and mutant bR, it was proposed that a unidirectional gate (a "proton diode") consisting of Glu194, Ser193 and Glu204 operates to prevent proton back-flow (Glu194 and Glu204 are implicated to be, or be associated with, a proton release/storage group in bR: [75,146]). In the ground-state of bR, hydrogen bonding between Ser193 and Glu204 leads to a conformation that prevents bulk water from accessing the interior of the bR channel. As a proton is released from the core of bR during the photocycle and move towards Glu194 and Glu 204, the hydrogen bond between Ser194 and Glu204 is weakened/broken, thereby allowing contact between the proton transferring water molecules in the bR interior (for an alternative view with focus on changes to $pK_a$ values rather than water access, see [146]). In this proposal, then, Ser193 acts as a gate that opens in response to proton release from bR, and closes otherwise to prevent proton back-flow. The making and breaking of water chains is thereby a central part of proton transport control, coupled to the photocycle.

### *8.3. Cytochrome P450 — water as a multi-functional and mechanistically coupled controlling element*

Cytochrome P450 enzymes (CYP) comprise a huge group of monooxygenase heme-proteins that are essential to many cellular processes in all known organisms. Their general function is the oxidation of a variety of hydrocarbon substrates during biosynthesis or degradation. Their involvement in drug deactivation in the human body has in particular turned CYPs into a well-studied pharmaceutical target. The mechanism of this enzyme has been extensively studied and reviewed (see for example [149] and references therein). Briefly, at the base of the enzyme active site is a low-spin ferric heme center that is 6-coordinated in the absence of substrate, with a water molecule occupying an axial position. Substrate binding to the active site displaces this coordinated water molecule, which leaves the active site along with any other waters molecules in the site. This leads to an activated 5-coordinate, high-spin ferric heme center with an increased reduction potential. This is followed by reduction of the heme by a reductase partner (varies depending on the CYP in question), leaving a ferrous center that favorably binds an $O_2$ molecule. Following a further reduction step, two protonation steps and O–O bond cleavage, the Fe(IV)-oxo species that oxidizes the substrate is obtained. During these final steps, however, protonation needs to be fine-tuned to avoid uncoupling, which would lead to hydrogen peroxide formation rather than O–O bond cleavage [150].

An especially interesting aspect with CYP for the current discussion is that water plays important and distinct roles in the catalytic cycle. As outlined below, water is present in specific places in the protein only when needed for specific functions, and excluded otherwise. It is an integral part of the catalytic cycle.

Though not a substrate as in PSII, the presence or absence of water in the CYP active site, including the water ligand to the heme center, tunes the spin, redox potential as well as $O_2$-binding affinity of the heme center. The large variety of channels found in different families of CYP, the dynamic nature of the water molecules in the active site, and the paths that they may take leaving the active site are indeed topics of much interest [151–153]. Furthermore, in order to avoid uncoupling, water chains leading to the active site are needed for protonation in some but not all steps of the catalytic cycle. Different mechanisms to synchronize water access to the catalytic cycle have been proposed.

With respect to the dehydration of the active site, it has been proposed that a conserved arginine residue that forms a salt-bridge with the 7-propionate of the heme center acts as a gate to a water channel. This "aqueduct" links the active site to the protein surface. [18,154]. Breaking of the salt-bridge through rotation of the arginine residue opens water access via the aqueduct. It appears that this salt-bridge closes the aqueduct in the substrate-bound state of CYP, after the desolvation and activation of the active site for reduction and $O_2$ binding, as outlined above (see also [153]). This closed state of the gate maintains the desolvation and activation. Sequence alignments of more than 500 homologues suggest that this aqueduct is present in many bacterial and mammalian CYPs, and that water permeability is controlled by the same arginine/7-proprionate gate gating mechanism (sometimes Lys or His replace Arg) [18,154]. The need for conformational change for aqueduct opening might also explain why the aqueduct has not always been observed [18,154,155]. A more active role for the gate in water expulsion has also been suggested [155].

To subsequently allow protonation of the oxygen-bound heme center, water access to the active site needs to be reestablished later in the catalytic cycle. From MD simulations and structural data [18,154], there is strong evidence for human CYP3A4 that the aqueduct is reopened upon binding of the reductase partner, allowing a water chain to the active site to reform. There is thereby a synchronization of water access

to the need for protonation of the heme-oxo-complex. The authors suggest that reductase binding weakens and consequently disrupts the salt-bridge between 7-propionate and Arg375. As a result, Arg375 rotates, thus opening the aqueduct and allowing for proton transfer to take place. Besides the aqueduct, another water chain may also be re-built after heme-oxo reduction to facilitate proton movement, possibly for the second protonation reaction at the active site [18,154]. In this case these ordered water molecules lead to (in CYP3A4) the Glu308 and The309 residues, and provide a hydrogen-bonded network for proton transfer with the threonine residue being the final proton deliverer. This is in agreement with findings for the analogous Asp251 and The252 residues in the bacterial CYP101A1 (CYPcam) [154,156,157], with the The252Ala mutation giving rise to uncoupling and formation of reactive oxygen species due to improper protonation [157,158].

The details of the water and proton transport mechanisms in CYP are still under investigation and discussion. There are a large number of channels in CYP in addition to those outlined here, with differences between the huge number of different CYPs [149,151]. Nevertheless, the apparently conserved gated aqueduct may provide a fine-tuned gating mechanism directly linking water access to the catalytic cycle. Water molecules can thus alternately act as the spin/redox-tuning or the proton conduction element, depending on the step in the cycle. There is clearly a close interplay between the protein environment and the water molecules, such that water becomes a dynamic and integral part of the functioning of the protein.

## 9. Concluding remarks

Water is clearly important for the functioning of PSII. Apart from being the very substrate for the enzyme, it is also vital for the transport of protons to and from the $Mn_4CaO_5$ cluster as well as other important co-factors and key residues in the enzyme. New possibilities and avenues for investigation have been opened by the latest crystal structure resolving water in the structure, but clearly much remains to be studied. The effects of the dynamic protein has been incorporated in some of the recent MD studies, but this will no doubt be much extended in the future to other investigations about, for example, energetics and redox properties. Studies of proton transfer will also benefit in this regard. The interaction between water molecules and the surrounding amino acid residues can have far-reaching effects, and the brief overview of the role of water in other, more well-studied enzymes gives a taste of this.

Reflecting on the role of water on this more general level, it becomes clear that water is much more than just a solvent. While a little special in being the substrate for PSII, mechanistically it can act to regulate and control the mechanistic function of the protein. This is of course performed in conjunction with changes in the protein itself, but it is worthwhile to consider protein residues and water as equally important in this regard. Indeed, as observed in CYP, the effect of water molecules can even be more direct, tuning the spin and redox properties of key co-factors in the enzyme. In PSII, this is a possibility that can be explored further. A good example is the observation that water is an axial ligand to seven of the 35 chlorophyll molecules in the crystal structure. Amongst these are both of the accessory chlorophylls in $P_{680}$ ($Chl_{D1}$ and $Chl_{D2}$), so it may be interesting to explore the effect of these water molecules, and whether any transient changes occur e.g. upon charge separation. It was for instance recently shown that the presence of an axial water ligand to $P_{D1}$ of the $P_{680}$ assembly in the D1-H198A mutant affected the reduction potential of $P_{680}$ [159].

In the context of proton transport, one can also pose the question: why are water molecules used for conduction at all, given that deprotonatable residues can also carry out proton transport via the Grotthuss mechanism? The logical answer is because water and amino acid residues serve different but complementary functions. While residues could in theory provide the required transport route, there would need to be a chain with a suitable $pK_a$ gradient in order for directional transport to be achieved. This could lead to highly charged regions in the protein, which may not be energetically favorable. For longer range proton transport, it may be difficult to establish a suitable chain based purely on amino acids. By contrast, a chain of water molecules can provide stretches of essentially isoenergetic paths for proton transport (of course still subject to charge and environmental effects from the protein surrounding). This becomes a more flexible and tunable pathway, as illustrated by the examples above. The very mobility of water molecules, while a potential hindrance for proton transport, is also a strength. Such proton pathway can be built/opened or broken/closed dynamically. By contrast, amino acid residues are arguably more suited to act as gates, or "traffic lights" in the proton highway.

While there may seem to be a degree of semantics in this discussion, if the role of water is elevated and considered more as an integral part of protein and enzyme function, deeper and interesting questions can be asked. For example, if a region in a crystal structure is devoid of water despite space being available, why is that so? Is it hydrophobicity, lack of access or high mobility that is the cause? In each case, are there underlying functional reasons, and how does the system behave under dynamic conditions? Similarly, the significance of the location of clusters, chains or even individual water molecules in relation to the protein environment can also be interrogated. By seeing water as an integral part of the protein, the inquiry and range of investigations can be broadened.

## Acknowledgements

The Swedish Energy Agency, the Knut and Alice Wallenberg Foundation, the Carl Tryggers Foundation for Scientific Research and the EU Program SOLAR-H2 (EU Contract 212508) are gratefully acknowledged for their financial support.

## References

[1] L.-X. Shi, M. Hall, C. Funk, W.P. Schröder, Photosystem II, a growing complex: updates on newly discovered components and low molecular mass proteins, Biochim. Biophys. Acta Bioenerg. 1817 (2012) 13–25.
[2] R.E. Blankenship, Molecular Mechanisms of Photosynthesis, Blackwell Science, Oxford, England, 2002.
[3] T.J. Wydrzynski, K. Satoh, Photosystem II: the light-driven water:plastoquinone oxidoreductase, in: Govindjee (Ed.), Advances in Photosynthesis and Respiration, Springer, The Netherlands, 2005.
[4] G. Renger, Primary Processes of Photosynthesis: Principles and Apparatus, RSC Publishing, Cambridge, England, 2008.
[5] F. Rappaport, B.A. Diner, Primary photochemistry and energetics leading to the oxidation of the (Mn)4Ca cluster and to the evolution of molecular oxygen in Photosystem II, Coord. Chem. Rev. 252 (2008) 259–272.
[6] H. Dau, M. Haumann, The manganese complex of photosystem II in its reaction cycle — basic framework and possible realization at the atomic level, Coord. Chem. Rev. 252 (2008) 273–295.
[7] H. Dau, I. Zaharieva, Principles, efficiency, and blueprint character of solar-energy conversion in photosynthetic water oxidation, Acc. Chem. Res. 42 (2009) 1861–1870.
[8] E.-M. Aro, Special Issue: Photosystem II, Biochim. Biophys. Acta Bioenerg. 1817 (2012).
[9] L.I. Krishtalik, Energetics of multielectron reactions — photosynthetic oxygen evolution, Biochim. Biophys. Acta 849 (1986) 162–171.
[10] P.E.M. Siegbahn, M. Lundberg, The mechanism for dioxygen formation in PSII studied by quantum chemical methods, Photochem. Photobiol. Sci. 4 (2005) 1035–1043.
[11] Y. Umena, K. Kawakami, J.-R. Shen, N. Kamiya, Crystal structure of oxygen-evolving photosystem II at a resolution of 1.9 Angstrom, Nature 473 (2011) 55–60.
[12] K.N. Ferreira, T.M. Iverson, K. Maghlaoui, J. Barber, S. Iwata, Architecture of the photosynthetic oxygen-evolving center, Science 303 (2004) 1831–1838.
[13] B. Loll, J. Kern, W. Saenger, A. Zouni, J. Biesiadka, Towards complete cofactor arrangement in the 3.0 angstrom resolution structure of photosystem II, Nature 438 (2005) 1040–1044.
[14] A. Guskov, J. Kern, A. Gabdulkhakov, M. Broser, A. Zouni, W. Saenger, Cyanobacterial photosystem II at 2.9-angstrom resolution and the role of quinones, lipids, channels and chloride, Nat. Struct. Mol. Biol. 16 (2009) 334–342.
[15] F.M. Ho, S. Styring, Access channels and methanol binding site to the CaMn4 cluster in Photosystem II based on solvent accessibility simulations, with implications for substrate water access, Biochim. Biophys. Acta Bioenerg. 1777 (2008) 140–153.

[16] F.M. Ho, Substrate and product channels in Photosystem II, in: T. Wydrzynski, W. Hillier (Eds.), Molecular Solar Fuels, The Royal Society of Chemistry, Cambridge, UK, 2012, pp. 208–248.
[17] E. Freier, S. Wolf, K. Gerwert, Proton transfer via a transient linear water-molecule chain in a membrane protein, Proc. Natl. Acad. Sci. U. S. A. 108 (2011) 11435–11439.
[18] D. Fishelovitch, S. Shaik, H.J. Wolfson, R. Nussinov, How does the reductase help to regulate the catalytic cycle of cytochrome P450 3A4 using the conserved water channel? J. Phys. Chem. B 114 (2010) 5964–5970.
[19] A. Marechal, P.R. Rich, Water molecule reorganization in cytochrome c oxidase revealed by FTIR spectroscopy, Proc. Natl. Acad. Sci. U. S. A. 108 (2011) 8634–8638.
[20] A.A. Arteni, G. Ajlani, E.J. Boekema, Structural organisation of phycobilisomes from Synechocystis sp strain PCC6803 and their interaction with the membrane, Biochim. Biophys. Acta Bioenerg. 1787 (2009) 272–279.
[21] J.W. Murray, K. Maghlaoui, J. Barber, The structure of allophycocyanin from *Thermosynechococcus elongatus* at 3.5 angstrom resolution, Acta Crystallographica Section F-Structural Biology and Crystallization Communications 63 (2007) 998–1002.
[22] T. Wydrzynski, W. Hillier, J. Messinger, On the functional significance of substrate accessibility in the photosynthetic water oxidation mechanism, Physiol. Plant. 96 (1996) 342–350.
[23] J.M. Anderson, Does functional photosystem II complex have an oxygen channel? FEBS Lett. 488 (2001) 1–4.
[24] A.W. Rutherford, Photosystem-II, the water-splitting enzyme, Trends Biochem. Sci. 14 (1989) 227–232.
[25] J.M. Anderson, W.S. Chow, Structural and functional dynamics of plant photosystem II, Philos. Trans. R. Soc. B-Biol. Sci. 357 (2002) 1421–1430.
[26] M.R.A. Blomberg, P.E.M. Siegbahn, Quantum chemistry as a tool in bioenergetics, Biochim. Biophys. Acta Bioenerg. 1797 (2010) 129–142.
[27] S. Cukierman, Et tu, Grotthuss! and other unfinished stories, Biochim. Biophys. Acta Bioenerg. 1757 (2006) 876–885.
[28] J.M.J. Swanson, C.M. Maupin, H.N. Chen, M.K. Petersen, J.C. Xu, Y.J. Wu, G.A. Voth, Proton solvation and transport in aqueous and biomolecular systems: insights from computer simulations, J. Phys. Chem. B 111 (2007) 4300–4314.
[29] C.A. Wraight, Chance and design — proton transfer in water, channels and bioenergetic proteins, Biochim. Biophys. Acta Bioenerg. 1757 (2006) 886–912.
[30] D. Marx, M.E. Tuckerman, J. Hutter, M. Parrinello, The nature of the hydrated excess proton in water, Nature 397 (1999) 601–604.
[31] J.M.J. Swanson, J. Simons, Role of charge transfer in the structure and dynamics of the hydrated proton, J. Phys. Chem. B 113 (2009) 5149–5161.
[32] R. Baron, J.A. McCammon, A. Mattevi, The oxygen-binding vs. oxygen-consuming paradigm in biocatalysis: structural biology and biomolecular simulation, Curr. Opin. Struct. Biol. 19 (2009) 672–679.
[33] Y. Wang, J. Cohen, W.F. Boron, K. Schulten, E. Tajkhorshid, Exploring gas permeability of cellular membranes and membrane channels with molecular dynamics, J. Struct. Biol. 157 (2007) 534–544.
[34] Y. Wang, S.A. Shaikh, E. Tajkhorshid, Exploring transmembrane diffusion pathways with molecular dynamics, Physiology 25 (2010) 142–154.
[35] F.M. Ho, Uncovering channels in photosystem II by computer modelling: current progress, future prospects, and lessons from analogous systems, Photosynth. Res. 98 (2008) 503–522.
[36] F.M. Ho, Structural and mechanistic investigations of photosystem II through computational methods, Biochim. Biophys. Acta Bioenerg. 1817 (2012) 106–120.
[37] J.W. Murray, J. Barber, Structural characteristics of channels and pathways in photosystem II including the identification of an oxygen channel, J. Struct. Biol. 159 (2007) 228–237.
[38] A. Gabdulkhakov, A. Guskov, M. Broser, J. Kern, F. Mueh, W. Saenger, A. Zouni, Probing the accessibility of the Mn4Ca cluster in Photosystem II: channels calculation, noble gas derivatization, and cocrystallization with DMSO, Structure 17 (2009) 1223–1234.
[39] S. Vassiliev, T. Zaraiskaya, D. Bruce, Exploring the energetics of water permeation in photosystem II by multiple steered molecular dynamics simulations, Biochim. Biophys. Acta Bioenerg. 1817 (2012) 1671–1678.
[40] H. Ishikita, W. Saenger, B. Loll, J. Biesiadka, E.W. Knapp, Energetics of a possible proton exit pathway for water oxidation in photosystem II, Biochemistry 45 (2006) 2063–2071.
[41] J.W. Murray, K. Maghlaoui, J. Kargul, M. Sugiura, J. Barber, Analysis of xenon binding to photosystem II by X-ray crystallography, Photosynth. Res. 98 (2008) 523–527.
[42] S. Vassiliev, T. Zaraiskaya, D. Bruce, Molecular dynamics simulations reveal highly permeable oxygen exit channels shared with water uptake channels in photosystem II, Biochim. Biophys. Acta Bioenerg. 1827 (2013) 1148–1155.
[43] H.X. Zhou, S.T. Wlodek, J.A. McCammon, Conformation gating as a mechanism for enzyme specificity, Proc. Natl. Acad. Sci. U. S. A. 95 (1998) 9280–9283.
[44] T.Y. Shen, K.H. Tai, R.H. Henchman, J.A. McCammon, Molecular dynamics of acetylcholinesterase, Acc. Chem. Res. 35 (2002) 332–340.
[45] P.I. Lario, N. Sampson, A. Vrielink, Sub-atomic resolution crystal structure of cholesterol oxidase: what atomic resolution crystallography reveals about enzyme mechanism and the role of the FAD cofactor in redox activity, J. Mol. Biol. 326 (2003) 1635–1650.
[46] J. Saam, I. Ivanov, M. Walther, H.G. Holzhutter, H. Kuhn, Molecular dioxygen enters the active site of 12/15-lipoxygenase via dynamic oxygen access channels, Proc. Natl. Acad. Sci. U. S. A. 104 (2007) 13319–13324.
[47] S. Vassiliev, P. Comte, A. Mahboob, D. Bruce, Tracking the flow of water through Photosystem II using molecular dynamics and streamline tracing, Biochemistry 49 (2010) 1873–1881.
[48] P.J. Basser, D.K. Jones, Diffusion-tensor MRI: theory, experimental design and data analysis — a technical review, NMR Biomed. 15 (2002) 456–467.
[49] S. Mori, P.C.M. van Zijl, Fiber tracking: principles and strategies — a technical review, NMR Biomed. 15 (2002) 468–480.
[50] R.A. Chylla, G. Garab, J. Whitmarsh, Evidence for slow turnover in a fraction of photosystem-II complexes in thylakoid membranes, Biochim. Biophys. Acta 894 (1987) 562–571.
[51] R.A. Chylla, J. Whitmarsh, Inactive photosystem-II complexes in leaves — turnover rate and quantitation, Plant Physiol. 90 (1989) 765–772.
[52] H. Dau, M. Haumann, Eight steps preceding O-O bond formation in oxygenic photo synthesis — a basic reaction cycle of the photosystem II manganese complex, Biochim. Biophys. Acta Bioenerg. 1767 (2007) 472–483.
[53] J. Lavergne, W. Junge, Proton release during the redox cycle of the water oxidase, Photosynth. Res. 38 (1993) 279–296.
[54] W. Junge, M. Haumann, R. Ahlbrink, A. Mulkidjanian, J. Clausen, Electrostatics and proton transfer in photosynthetic water oxidation, Philos. Trans. R. Soc. B-Biol. Sci. 357 (2002) 1407–1418.
[55] F. Rappaport, J. Lavergne, Proton release during successive oxidation steps of the photosynthetic water oxidation process — stoichiometries and ph-dependence, Biochemistry 30 (1991) 10004–10012.
[56] E.M. Sproviero, J.A. Gascon, J.P. McEvoy, G.W. Brudvig, V.S. Batista, Computational studies of the $O_2$-evolving complex of photosystem II and biomimetic oxomanganese complexes, Coord. Chem. Rev. 252 (2008) 395–415.
[57] M. Haumann, P. Liebisch, C. Muller, M. Barra, M. Grabolle, H. Dau, Photosynthetic $O_2$ formation tracked by time-resolved X-ray experiments, Science 310 (2005) 1019–1021.
[58] L. Gerencser, H. Dau, Water oxidation by photosystem II: $H_2O$–$D_2O$ exchange and the influence of pH support formation of an intermediate by removal of a proton before dioxygen creation, Biochemistry 49 (2010) 10098–10106.
[59] F. Rappaport, M. Blanchard-desce, J. Lavergne, Kinetics of electron-transfer and electrochromic change during the redox transitions of the photosynthetic oxygen-evolving complex, Biochim. Biophys. Acta Bioenerg. 1184 (1994) 178–192.
[60] G. Bernát, F. Morvaridi, Y. Feyziyev, S. Styring, pH dependence of the four individual transitions in the catalytic S-cycle during photosynthetic oxygen evolution, Biochemistry 41 (2002) 5830–5843.
[61] H. Suzuki, M. Sugiura, T. Noguchi, pH dependence of the flash-induced S-state transitions in the oxygen-evolving center of photosystem II from *Thermosynechoccocus elongatus* as revealed by Fourier transform infrared spectroscopy, Biochemistry 44 (2005) 1708–1718.
[62] T. Noguchi, H. Suzuki, M. Tsuno, M. Sugiura, C. Kato, Time-resolved infrared detection of the proton and protein dynamics during photosynthetic oxygen evolution, Biochemistry 51 (2012) 3205–3214.
[63] A. Klauss, M. Haumann, H. Dau, Alternating electron and proton transfer steps in photosynthetic water oxidation, Proc. Natl. Acad. Sci. U. S. A. 109 (2012) 16035–16040.
[64] J. Sjoholm, S. Styring, K.G.V. Havelius, F.M. Ho, Visible light induction of an electron paramagnetic resonance split signal in Photosystem II in the S-2 state reveals the importance of charges in the oxygen-evolving center during catalysis: a unifying model, Biochemistry 51 (2012) 2054–2064.
[65] M.P. Klein, K. Sauer, V.K. Yachandra, Perspectives on the structure of the photosynthetic oxygen-evolving manganese complex and its relation to the kok cycle, Photosynth. Res. 38 (1993) 265–277.
[66] M. Haumann, W. Junge, Photosynthetic water oxidation: a simplex-scheme of its partial reactions, Biochim. Biophys. Acta Bioenerg. 1411 (1999) 86–91.
[67] J. Barber, K. Ferreira, K. Maghlaoui, S. Iwata, Structural model of the oxygen-evolving centre of photosystem II with mechanistic implications, Phys. Chem. Chem. Phys. 6 (2004) 4737–4742.
[68] R.J. Debus, The catalytic manganese cluster: protein ligation, in: T. Wydrzynski, K. Satoh (Eds.), Photosystem II: The Light-driven Water:Plastoquinone Oxidoreductase, Springer, The Netherlands, 2005, pp. 261–284.
[69] R.J. Service, W. Hillier, R.J. Debus, Evidence from FTIR difference spectroscopy of an extensive network of hydrogen bonds near the oxygen-evolving Mn4Ca cluster of Photosystem II involving D1–Glu, 65, D2–Glu312, and D1–Glu329, Biochemistry 49 (2010) 6655–6669.
[70] A.N. Bondar, H. Dau, Extended protein/water H-bond networks in photosynthetic water oxidation, Biochim. Biophys. Acta Bioenerg. 1817 (2012) 1177–1190.
[71] T. Shutova, V.V. Klimov, B. Andersson, G. Samuelsson, A cluster of carboxylic groups in PsbO protein is involved in proton transfer from the water oxidizing complex of Photosystem II, Biochim. Biophys. Acta Bioenerg. 1767 (2007) 434–440.
[72] T. Shutova, H. Kenneweg, J. Buchta, J. Nikitina, V. Terentyev, S. Chernyshov, B. Andersson, S.I. Allakhverdiev, V.V. Klimov, H. Dau, W. Junge, G. Samuelsson, The photosystem II-associated Cah3 in Chlamydomonas enhances the O-2 evolution rate by proton removal, EMBO J. 27 (2008) 782–791.
[73] F.M. Ho, Molecular dynamics simulations of a putative $H^+$ pathway in Photosystem II, in: T. Kuang, C. Lu, L. Zhang (Eds.), Photosynthesis Research for Food, Fuel and Future: 15th International Conference on Photosynthesis, Zhejiang University Press and Springer, Beijing, China, 2010.
[74] K. Linke, F.M. Ho, Investigation of a putative hotspot for proton transport in Photosystem II through parallel *in vivo* mutagenesis and *in silico* molecular dynamics studies, (in preparation).
[75] F. Garczarek, L.S. Brown, J.K. Lanyi, K. Gerwert, Proton binding within a membrane protein by a protonated water cluster, Proc. Natl. Acad. Sci. U. S. A. 102 (2005) 3633–3638.
[76] P. Phatak, N. Ghosh, H.B. Yu, Q. Cui, M. Elstner, Amino acids with an intermolecular proton bond as proton storage site in bacteriorhodopsin, Proc. Natl. Acad. Sci. U. S. A. 105 (2008) 19672–19677.

[77] M.R.A. Blomberg, P.E.M. Siegbahn, The mechanism for proton pumping in cytochrome c oxidase from an electrostatic and quantum chemical perspective, Biochim. Biophys. Acta Bioenerg. 1817 (2012) 495–505.
[78] H.J. Lee, E. Svahn, J.M.J. Swanson, H. Lepp, G.A. Voth, P. Brzezinski, R.B. Gennis, Intricate role of water in proton transport through cytochrome c oxidase, J. Am. Chem. Soc. 132 (2010) 16225–16239.
[79] C. Knight, G.A. Voth, The curious case of the hydrated proton, Acc. Chem. Res. 45 (2012) 101–109.
[80] J. Messinger, T. Noguchi, J. Yano, Photosynthetic $O_2$ evolution, in: T. Wydrzynski, W. Hillier (Eds.), Molecular Solar Fuels, The Royal Society of Chemistry, Cambridge, UK, 2012.
[81] H. Dau, I. Zaharieva, M. Haumann, Recent developments in research on water oxidation by photosystem II, Curr. Opin. Chem. Biol. 16 (2012) 3–10.
[82] G. Renger, Mechanism of light induced water splitting in Photosystem II of oxygen evolving photosynthetic organisms, Biochim. Biophys. Acta Bioenerg. 1817 (2012) 1164–1176.
[83] E.M. Sproviero, J.A. Gascon, J.P. McEvoy, G.W. Brudvig, V.S. Batista, Quantum mechanics/molecular mechanics study of the catalytic cycle of water splitting in photosystem II, J. Am. Chem. Soc. 130 (2008) 3428–3442.
[84] C.W. Hoganson, N. LydakisSimantiris, X.S. Tang, C. Tommos, K. Warncke, G.T. Babcock, B.A. Diner, J. McCracken, S. Styring, A hydrogen-atom abstraction model for the function of Y-Z in photosynthetic oxygen evolution, Photosynth. Res. 46 (1995) 177–184.
[85] C.W. Hoganson, G.T. Babcock, A metalloradical mechanism for the generation of oxygen from water in photosynthesis, Science 277 (1997) 1953–1956.
[86] M.H.V. Huynh, T.J. Meyer, Proton-coupled electron transfer, Chem. Rev. 107 (2007) 5004–5064.
[87] D.R. Weinberg, C.J. Gagliardi, J.F. Hull, C.F. Murphy, C.A. Kent, B.C. Westlake, A. Paul, D.H. Ess, D.G. McCafferty, T.J. Meyer, Proton-coupled electron transfer, Chem. Rev. 112 (2012) 4016–4093.
[88] R. Ahlbrink, M. Haumann, D. Cherepanov, O. Bogershausen, A. Mulkidjanian, W. Junge, Function of tyrosine Z in water oxidation by photosystem II: electrostatical promotor instead of hydrogen abstractor, Biochemistry 37 (1998) 1131–1142.
[89] P.E.M. Siegbahn, M.R.A. Blomberg, Quantum chemical studies of proton-coupled electron transfer in metalloenzymes, Chem. Rev. 110 (2010) 7040–7061.
[90] P.E.M. Siegbahn, Recent theoretical studies of water oxidation in photosystem II, J. Photochem. Photobiol. B Biol. 104 (2011) 94–99.
[91] P.E.M. Siegbahn, Mechanisms for proton release during water oxidation in the S-2 to S-3 and S-3 to S-4 transitions in photosystem II, Phys. Chem. Chem. Phys. 14 (2012) 4849–4856.
[92] I. Rivalta, M. Amin, S. Luber, S. Vassiliev, R. Pokhrel, Y. Umena, K. Kawakami, J.R. Shen, N. Kamiya, D. Bruce, G.W. Brudvig, M.R. Gunner, V.S. Batista, Structural-functional role of chloride in Photosystem II, Biochemistry 50 (2011) 6312–6315.
[93] P.L. Dilbeck, H.J. Hwang, I. Zaharieva, L. Gerencser, H. Dau, R.L. Burnap, The D1-D61N mutation in *Synechocystis* sp PCC 6803 allows the observation of pH-sensitive intermediates in the formation and release of O-2 from Photosystem II, Biochemistry 51 (2012) 1079–1091.
[94] M. Hundelt, A.M.A. Hays, R.J. Debus, W. Junge, Oxygenic Photosystem II: the mutation D1-D61N in *Synechocystis* sp. PCC 6803 retards S-state transitions without affecting electron transfer from $Y_Z$ to $P_{680}^{+}$, Biochemistry 37 (1998) 14450–14456.
[95] K.A. Campbell, J.M. Peloquin, B.A. Diner, X.S. Tang, D.A. Chisholm, R.D. Britt, The tau-nitrogen of D2 histidine 189 is the hydrogen bond donor to the tyrosine radical Y-D(center dot) of photosystem II, J. Am. Chem. Soc. 119 (1997) 4787–4788.
[96] S. Styring, J. Sjöholm, F. Mamedov, Two tyrosines that changed the world: interfacing the oxidizing power of photochemistry to water splitting in photosystem II, Biochim. Biophys. Acta Bioenerg. 1817 (2012) 76–87.
[97] A.W. Rutherford, A. Boussac, P. Faller, The stable tyrosyl radical in Photosystem II: why D? Biochim. Biophys. Acta Bioenerg. 1655 (2004) 222–230.
[98] K. Brettel, E. Schlodder, H.T. Witt, Nanosecond reduction kinetics of photooxidized chlorophyll-alpha-II (p-680) in single flashes as a probe for the electron pathway, h + -release and charge accumulation in the o-2-evolving complex, Biochim. Biophys. Acta 766 (1984) 403–415.
[99] G. Christen, F. Reifarth, G. Renger, On the origin of the '35-μs kinetics' of $P680^{+\cdot}$ reduction in photosystem II with an intact water oxidising complex, FEBS Lett. 429 (1998) 49–52.
[100] I. Vass, S. Styring, Ph-dependent charge equilibria between tyrosine-D and the S-states in Photosystem.2. Estimation of relative midpoint redox potentials, Biochemistry 30 (1991) 830–839.
[101] S. Styring, A.W. Rutherford, In the oxygen-evolving complex of Photosystem II the S0 state is oxidized to the S1 state by D + (Signal-Iislow), Biochemistry 26 (1987) 2401–2405.
[102] P. Faller, R.J. Debus, K. Brettel, M. Sugiura, A.W. Rutherford, A. Boussac, Rapid formation of the stable tyrosyl radical in photosystem II, Proc. Natl. Acad. Sci. U. S. A. 98 (2001) 14368–14373.
[103] P. Faller, A.W. Rutherford, R.J. Debus, Tyrosine D oxidation at cryogenic temperature in photosystem II, Biochemistry 41 (2002) 12914–12920.
[104] K. Saito, A.W. Rutherford, H. Ishikita, Mechanism of tyrosine D in Photosystem II, Proc. Natl. Acad. Sci. U. S. A. 110 (2013) 7690–7695.
[105] G.T. Babcock, B.A. Barry, R.J. Debus, C.W. Hoganson, M. Atamian, L. McIntosh, I. Sithole, C.F. Yocum, Water oxidation in photosystem.2. from radical chemistry to multielectron chemistry, Biochemistry 28 (1989) 9557–9565.
[106] R.J. Boerner, K.A. Bixby, A.P. Nguyen, G.H. Noren, R.J. Debus, B.A. Barry, Removal of stable tyrosine radical d + affects the structure or redox properties of tyrosine-z in manganese-depleted photosystem-II particles from synechocystis 6803, J. Biol. Chem. 268 (1993) 1817–1823.
[107] G.A. Ananyev, I. Sakiyan, B.A. Diner, G.C. Dismukes, A functional role for tyrosine-D in assembly of the inorganic core of the water oxidase complex of photosystem II and the kinetics of water oxidation, Biochemistry 41 (2002) 974–980.
[108] B.A. Diner, F. Rappaport, Structure, dynamics, and energetics of the primary photochemistry of photosystem II of oxygenic photosynthesis, Annu. Rev. Plant Biol. 53 (2002) 551–580.
[109] M. Szczepaniak, M. Sugiura, A.R. Holzwarth, The role of TyrD in the electron transfer kinetics in Photosystem II, Biochim. Biophys. Acta Bioenerg. 1777 (2008) 1510–1517.
[110] F. Muh, C. Glockner, J. Hellmich, A. Zouni, Light-induced quinone reduction in photosystem II, Biochim. Biophys. Acta Bioenerg. 1817 (2012) 44–65.
[111] J. Xiong, S. Subramaniam, Govindjee, Modeling of the D1/D2 proteins and cofactors of the photosystem II reaction center: implications for herbicide and bicarbonate binding, Protein Sci. 5 (1996) 2054–2073.
[112] D. Shevela, J.J. Eaton-Rye, J.R. Shen, Govindjee, Photosystem II and the unique role of bicarbonate: a historical perspective, Biochim. Biophys. Acta Bioenerg. 1817 (2012) 1134–1151.
[113] M.Y. Okamura, M.L. Paddock, M.S. Graige, G. Feher, Proton and electron transfer in bacterial reaction centers, Biochim. Biophys. Acta Bioenerg. 1458 (2000) 148–163.
[114] E. Nabedryk, J. Breton, Coupling of electron transfer to proton uptake at the Q(B) site of the bacterial reaction center: a perspective from FTIR difference spectroscopy, Biochim. Biophys. Acta Bioenerg. 1777 (2008) 1229–1248.
[115] J. Koepke, E.-M. Krammer, A.R. Klingen, P. Sebban, G.M. Ullmann, G. Fritzsch, pH modulates the quinone position in the photosynthetic reaction center from Rhodobacter sphaeroides in the neutral and charge separated states, J. Mol. Biol. 371 (2007) 396–409.
[116] M.L. Paddock, G. Feher, M.Y. Okamura, Proton transfer pathways and mechanism in bacterial reaction centers, FEBS Lett. 555 (2003) 45–50.
[117] M.H.B. Stowell, T.M. McPhillips, D.C. Rees, S.M. Soltis, E. Abresch, G. Feher, Light-induced structural changes in photosynthetic reaction center: implications for mechanism of electron-proton transfer, Science 276 (1997) 812–816.
[118] Z.Y. Zhu, M.R. Gunner, Energetics of quinone-dependent electron and proton transfers in Rhodobacter sphaeroides photosynthetic reaction centers, Biochemistry 44 (2005) 82–96.
[119] E. Takahashi, C.A. Wraight, A crucial role for aspl213 in the proton-transfer pathway to the secondary quinone of reaction centers from rhodobacter-sphaeroides, Biochim. Biophys. Acta 1020 (1990) 107–111.
[120] R. Takahashi, A. Boussac, M. Sugiura, T. Noguchi, Structural coupling of a tyrosine side chain with the non-heme iron center in Photosystem II as revealed by light-induced Fourier transform infrared difference spectroscopy, Biochemistry 48 (2009) 8994–9001.
[121] V. Petrouleas, A.R. Crofts, The iron–quinone acceptor complex, in: T.J. Wydrzynski, K. Satoh (Eds.), Photosystem II: The Light-Driven Water:Plastoquinone Oxidoreductase, Springer, The Netherlands, 2005, pp. 177–206.
[122] C. Berthomieu, R. Hienerwadel, Iron coordination in photosystem II: interaction between bicarbonate and the Q(B) pocket studied by Fourier transform infrared spectroscopy, Biochemistry 40 (2001) 4044–4052.
[123] K. Saito, A.W. Rutherford, H. Ishikita, Mechanism of proton-coupled quinone reduction in Photosystem II, Proc. Natl. Acad. Sci. U. S. A. 110 (2013) 954–959.
[124] N. Ohad, J. Hirschberg, A similar structure of the herbicide binding-site in Photosystem-II of plants and cyanobacteria is demonstrated by site specific mutagenesis of the psbA gene, Photosynth. Res. 23 (1990) 73–79.
[125] N. Ohad, J. Hirschberg, Mutations in the D1 subunit of Photosystem-II distinguish between quinone and herbicide binding-sites, Plant Cell 4 (1992) 273–282.
[126] A.L. Etienne, J.M. Ducruet, G. Ajlani, C. Vernotte, Comparative-studies on electron-transfer in Photosystem-II of herbicide-resistant mutants from different organisms, Biochim. Biophys. Acta 1015 (1990) 435–440.
[127] M. DallaChiesa, G. Friso, Z. Deak, I. Vass, J. Barber, P.J. Nixon, Reduced turnover of the D1 polypeptide and photoactivation of electron transfer in novel herbicide resistant mutants of *Synechocystis* sp. PCC 6803, Eur. J. Biochem. 248 (1997) 731–740.
[128] W. Oettmeier, Herbicide resistance and supersensitivity in photosystem II, Cell Mol. Life Sci. 55 (1999) 1255–1277.
[129] H. Kless, M. Orenshamir, S. Malkin, L. McIntosh, M. Edelman, The d–e region of the d1 protein is involved in multiple quinone and herbicide interactions in photosystem-II, Biochemistry 33 (1994) 10501–10507.
[130] B.L. de Groot, H. Grubmüller, The dynamics and energetics of water permeation and proton exclusion in aquaporins, Curr. Opin. Struct. Biol. 15 (2005) 176–183.
[131] B. Roux, K. Schulten, Computational studies of membrane channels, Structure 12 (2004) 1343–1351.
[132] G.D. Hu, L.Y. Chen, J.H. Wang, Insights into the mechanisms of the selectivity filter of Escherichia coli aquaporin Z, J. Mol. Model. 18 (2012) 3731–3741.
[133] J.S. Jiang, B.V. Daniels, D. Fu, Crystal structure of AqpZ tetramer reveals two distinct Arg-189 conformations associated with water permeation through the narrowest constriction of the water-conducting channel, J. Biol. Chem. 281 (2006) 454–460.
[134] L. Xin, H.B. Su, C.H. Nielsen, C.Y. Tang, J. Torres, Y.G. Mu, Water permeation dynamics of AqpZ: a tale of two states, Biochim. Biophys. Acta Biomembr. 1808 (2011) 1581–1586.
[135] S. Tornroth-Horsefield, Y. Wang, K. Hedfalk, U. Johanson, M. Karlsson, E. Tajkhorshid, R. Neutze, P. Kjellbom, Structural mechanism of plant aquaporin gating, Nature 439 (2006) 688–694.

[136] I. Johansson, M. Karlsson, V.K. Shukla, M.J. Chrispeels, C. Larsson, P. Kjellbom, Water transport activity of the plasma membrane aquaporin PM28A is regulated by phosphorylation, Plant Cell 10 (1998) 451–459.
[137] H. Khandelia, M.O. Jensen, O.G. Mouritsen, To gate or not to gate: using molecular dynamics simulations to morph gated plant aquaporins into constitutively open conformations, J. Phys. Chem. B 113 (2009) 5239–5244.
[138] M. Nyblom, A. Frick, Y. Wang, M. Ekvall, K. Hallgren, K. Hedfalk, R. Neutze, E. Tajkhorshid, S. Tornroth-Horsefield, Structural and functional analysis of SoPIP2;1 mutants adds insight into plant aquaporin gating, J. Mol. Biol. 387 (2009) 653–668.
[139] M. Zelenina, S. Zelenin, A.A. Bondar, H. Brismar, A. Aperia, Water permeability of aquaporin-4 is decreased by protein kinase C and dopamine, Am. J. Physiol. Ren. Physiol. 283 (2002) F309–F318.
[140] K. Eto, Y. Noda, S. Horikawa, S. Uchida, S. Sasaki, Phosphorylation of aquaporin-2 regulates its water permeability, J. Biol. Chem. 285 (2010) 40777–40784.
[141] C. Kandt, K. Gerwert, J. Schlitter, Water dynamics simulation as a tool for probing proton transfer pathways in a heptahelical membrane protein, Proteins 58 (2005) 528–537.
[142] J.K. Lanyi, Bacteriorhodopsin, Annu. Rev. Physiol. 66 (2004) 665–688.
[143] J.K. Lanyi, Proton transfers in the bacteriorhodopsin photocycle, Biochim. Biophys. Acta Bioenerg. 1757 (2006) 1012–1018.
[144] S. Wolf, E. Freier, K. Gerwert, How does a membrane protein achieve a vectorial proton transfer via water molecules? Chemphyschem 9 (2008) 2772–2778.
[145] T. Hirai, S. Subramaniam, J.K. Lanyi, Structural snapshots of conformational changes in a seven-helix membrane protein: lessons from bacteriorhodopsin, Curr. Opin. Struct. Biol. 19 (2009) 433–439.
[146] P. Goyal, N. Ghosh, P. Phatak, M. Clemens, M. Gaus, M. Elstner, Q. Cui, Proton storage site in bacteriorhodopsin: new insights from quantum mechanics/molecular mechanics simulations of microscopic pK(a) and infrared spectra, J. Am. Chem. Soc. 133 (2011) 14981–14997.
[147] T. Wang, A.O. Sessions, C.S. Lunde, S. Rouhani, R.M. Glaeser, Y. Duan, M.T. Facciotti, Deprotonation of D96 in bacteriorhodopsin opens the proton uptake pathway, Structure 21 (2013) 290–297.
[148] S. Wolf, E. Freier, M. Potschies, E. Hofmann, K. Gerwert, Directional proton transfer in membrane proteins achieved through protonated protein-bound water molecules: a proton diode, Angew. Chem. Int. Ed. 49 (2010) 6889–6893.
[149] P.R. Ortiz de Montellano, Cytochrome P450: Structure, Mechanism, and Biochemistry, Kluwer Academic/Plenum Publishers, New York, 2005.
[150] T.M. Markris, I. Denisov, I. Schlichting, S.G. Sligar, Activation of molecular oxygen by cytochrome P450, in: P.R. Ortiz de Montellano (Ed.), Cytochrome P450: Structure, Mechanism, and Biochemistry, Kluwer Academic/Plenum Publishers, New York, 2005, pp. 149–182.
[151] V. Cojocaru, P.J. Winn, R.C. Wade, The ins and outs of cytochrome P450s, Biochim. Biophys. Acta Gen. Subj. 1770 (2007) 390–401.
[152] P. Rydberg, T.H. Rod, L. Olsen, U. Ryde, Dynamics of water molecules in the active-site cavity of human cytochromes P450, J. Phys. Chem. B 111 (2007) 5445–5457.
[153] Y.L. Miao, J. Baudry, Active-site hydration and water diffusion in cytochrome P450cam: a highly dynamic process, Biophys. J. 101 (2011) 1493–1503.
[154] T.I. Oprea, G. Hummer, A.E. Garcia, Identification of a functional water channel in cytochrome P450 enzymes, Proc. Natl. Acad. Sci. U. S. A. 94 (1997) 2133–2138.
[155] T. Hayashi, K. Harada, K. Sakurai, H. Shimada, S. Hirota, A role of the heme-7-propionate side chain in cytochrome P450cam as a gate for regulating the access of water molecules to the substrate-binding site, J. Am. Chem. Soc. 131 (2009) 1398-+.
[156] I. Schlichting, J. Berendzen, K. Chu, A.M. Stock, S.A. Maves, D.E. Benson, B.M. Sweet, D. Ringe, G.A. Petsko, S.G. Sligar, The catalytic pathway of cytochrome P450cam at atomic resolution, Science 287 (2000) 1615–1622.
[157] R. Raag, S.A. Martinis, S.G. Sligar, T.L. Poulos, Crystal-structure of the cytochrome-p-450cam active-site mutant thr252ala, Biochemistry 30 (1991) 11420–11429.
[158] S.A. Martinis, W.M. Atkins, P.S. Stayton, S.G. Sligar, A conserved residue of cytochrome-p-450 is involved in heme-oxygen stability and activation, J. Am. Chem. Soc. 111 (1989) 9252–9253.
[159] K. Saito, J.R. Shen, H. Ishikita, Influence of the axial ligand on the cationic properties of the chlorophyll pair in Photosystem II from *Thermosynechococcus vulcanus*, Biophys. J. 102 (2012) 2634–2640.